Response to reviewer comments for the manuscript: **Impact of El Niño Southern Oscillation on the interannual variability of methane and tropospheric ozone** by **Rowlinson et al.**

We thank the two reviewers for their detailed feedback on our manuscript. We have now carefully revised the manuscript according to all the comments provided. To guide the review process we have copied the reviewer comments below (in black) and provided our responses (in blue).

Responses to reviewer #1:

Reviewer Summary:
In this paper, the authors document the results of model experiments analyzing the influence of ENSO on interannual variability of carbon monoxide, tropospheric ozone, hydroxyl radical and resulting impact on radiative effects and methane variability. The paper is generally well-organized and addresses scientific questions within the scope of ACP. My two main concerns are: a) the ability of the model to capture observations during ENSO years has not been explicitly demonstrated and b) results from previous studies (both model and observational) on the influence of ENSO on tropospheric ozone have not been considered (though studies on IAV of CO have been considered). These issues are highlighted below with specific suggestions on further improving the manuscript.

Authors' response: We would like to thank the reviewer for the positive and constructive comments on our manuscript. We agree that the two major concerns raised are important and improve the manuscript. We have now substantially revised our study to address both major concerns. In particular:

a) We conducted further evaluation of the model in order to demonstrate its ability to capture ENSO events. This has been done using the Ozone ENSO Index (OEI) proposed by Ziemke et al. (2010) and by comparing regional tropospheric O_3 changes during El Niño events to previous studies. These developments are explained in detail below.
b) We included considerably more discussion of the influence of El Niño on tropospheric O_3, detailing how our results compare with previous literature and providing explanations for the responses simulated in our model.

Specific Comments:
Abstract: To me, the first sentence of the abstract gives the impression that the focus of this study is the analysis of methane trends and variability which is currently being intensely debated in the literature (Turner et al., 2019; Nisbet et al., 2019). Unless I misunderstood, the paper is geared towards analysing the impact of ENSO on carbon monoxide, tropospheric ozone, hydroxyl radical as well as methane. The influence of ENSO on methane variability is discussed here but a full analysis of the methane growth rate is not performed in this study. Lines 45-47 better reflect the analyses performed here. The first couple of sentences should be revised so that they accurately represent the focus of this study which I understand to be ENSO driven changes in atmospheric composition and their impacts rather than just methane growth rate.

Authors' response: We thank the reviewer for this point and we agree that the abstract needs to be reformulated to avoid any confusion and to better summarise the findings of the paper.
We have now revised the abstract to more accurately convey the scope of the paper:

Changes in manuscript:
L43-46

"The interannual variability of greenhouse gases methane (CH_4) and tropospheric ozone (O_3) is largely driven by natural variations in global emissions and meteorology. The El Niño Southern Oscillation (ENSO) is known to influence fire occurrence, wetland emission and atmospheric circulation, affecting sources and sinks of CH_4 and tropospheric O_3, but there are still important uncertainties associated with the exact mechanism and magnitude of this effect."

Section 2.1: How does the model calculate biogenic VOC emissions? Given that VOC oxidation is an important source of CO (about 15% according to Duncan et al. 2007), I would imagine that variability in VOC emissions (driven by variations in meteorology, radiation, land-use, CO2) (Lathiere et al., 2005) would have some impact on CO IAV.

Authors' response: In our study, biogenic VOC emissions are not calculated in the model but read in from the MEGAN-MACC biogenic emissions inventory. The emissions are fixed-year so we do not simulate the effect of BVOC IAV on CO IAV, however monthly and seasonal variability is accounted for. We have now clarified this in the text.

Changes in manuscript:
L141-142
"Monthly varying biogenic VOC emissions are from the MEGAN-MACC emissions inventory for reference year 2000, calculated from the Model of Emissions of Gases and Aerosols from Nature (MEGANv2) (Sindelarova et al., 2014)."

We now discuss this in Section 4.1 as a possible explanation for the slightly lower CO IAV calculated compared to Voulgarakis et al. (2015), however although the seasonal variability of BVOC emissions is high (17-25%), studies have found the interannual variation to be relatively minor (2-4%) (Naik et al., 2004; Lathière et al., 2005). Therefore, although we acknowledge that we do not account for CO IAV from BVOC IAV, the impact is likely small. In the text we now discuss the importance of BVOC oxidation as a source of CO and the relatively small interannual variability of BVOC emissions.

Changes in manuscript:
L296-299
"The slightly lower estimate here may be a result of the fixed-year BVOC emissions, removing the effect of IAV of biogenic emissions on CO IAV. BVOC oxidation is estimated to contribute 15% of the total source of CO (Duncan et al., 2007), however the IAV of BVOC emissions has been found to be relatively small, ~2-4% (Naik et al., 2004; Lathière et al., 2005)."

L133-134: Emissions of "all source of methane have been included in the model." Could you please elaborate on which sources of methane emissions have been included in the model?

Authors' response: We agree it is important to be more specific here, so we have expanded on this statement in the text.

Changes in manuscript:
L142-146
"The CH_4 inventory was produced by (McNorton et al., 2016b), with wetland emissions derived from the Joint UK Land Environment Simulator (JULES) and biomass burning emissions from GFEDv4 (Randerson et al., 2017). These are then combined with anthropogenic emissions from EDGARv3.2, paddy field emissions from Yan et al. (2009) and termite, wild animal, mud volcano, hydrate and ocean emissions from Matthews and Fung (1987) (McNorton et al., 2016b)."

L135: Replace nitrous oxide (which is N2O) with nitrogen oxide.

Authors' response: Thank you for pointing out the mistake. This has now been corrected.

L137-139: What emissions does JULES simulate? Wetlands? Agriculture? Please clarify.

Authors' response: This has now been addressed in the reply to a previous comment and the addition of new text at **L142-146**.

Section 3: Given that the model is being used to analyse the impact of El Nino, in addition to the climatological evaluation discussed in this section, a more focused evaluation against measurements in El Nino years would more appropriately build confidence in the model's ability to capture features unique to conditions in these years.

Authors' response: We agree that this is an important point that would add confidence in the model and our conclusions. We now clarify in section 2.1 that our model is driven by ECMWF reanalysis, which has previously been shown to be able to represent ENSO events.

Changes in manuscript:
L133-135
"ECMWF ERA-Interim reanalyses have been shown to have good skill in capturing Madden-Julian Oscillation (MJO) events which in turn impact the onset of ENSO events (Dee et al., 2011), giving confidence that the model competently represents El Niño meteorological conditions."

We have now also compared simulated tropospheric O_3 response to El Niño events against observed responses in literature. We calculate an Ozone ENSO Index (OEI) based on Ziemke et al. (2010), which yields a response of +2.8 DU in the model. This compares with a +2.4 DU response in observations given in Ziemke et al. (2010). We have also added a new figure in the supplementary material showing regional response in total O_3 column and compared this to findings of Zhang et al. (2015) (Fig. S5).

Changes in manuscript:
L197-204
"We have also assessed the capability of TOMCAT-GLOMAP to simulate observed responses to El Niño events. Ziemke et al. (2010) derived an O_3 ENSO index using satellite observations, finding that for a +1K change in the Nino 3.4 index, there was a 2.4 DU increase in the OEI. In TOMCAT-GLOMAP, we calculate a 2.8 DU increase per +1K in the Nino 3.4, indicating a slightly larger but comparable response to El Niño events. The regional response of tropospheric O_3 to El Niño was evaluated against an analysis using various observations and a chemistry-climate model in Zhang et al. (2015). That study observed increased total O_3 column in the North Pacific, southern USA, north-eastern Africa and East Asia, with decreases over central Europe and the North Atlantic. All of these observed responses were present in TOMCAT-GLOMAP simulations, except with a slight increase in TOC in central Europe and a simulated decrease in Western Europe and East Atlantic (Fig. S5). "

L167-168: Are averaging kernels applied to model output for evaluation against satellite observations? Please clarify for MOPITT CO and OMI ozone.

Authors' response: Averaging kernels were applied to the model output before they could be compared against satellite retrievals. This is now clarified in detail in the supplementary, with an explanatory sentence added in section 3.

Changes in manuscript:
L176-178
"MOPITT satellite retrievals have been used to evaluate CO at 800 hPa and 500 hPa (Emmons et al., 2004) and are shown in Fig. S1 and S2, respectively, along with a description of satellite product and averaging kernels applied to the model output."

L190-191: It is stated on L139-140 that surface methane concentrations are scaled in the model to observed values. It is therefore not surprising that the model performs well near the surface for methane. I think this sentence should be caveated.

Authors' response: We thank the reviewer for this observation as this is an important point which was not made clear in the original manuscript. The scaling in TOMCAT-GLOMAP affects only the simulated global mean surface methane concentration, scaling this value to the observed global mean surface concentration. The spatial distribution and vertical transport of methane is still simulated and therefore relevant to be evaluated. The description of the methane scaling has been revised:

Changes in manuscript:
L146-148
"The global mean surface CH_4 mixing ratio is scaled in TOMCAT-GLOMAP to a best-estimate based on observed global surface CH_4 mean concentration (McNorton et al., 2016a; Dlugokencky, 2019)."

However, we agree that the statement on model performance for methane simulation should be caveated. We have revised the statement now on L215-217:

Changes in manuscript:
L219-222
"Absolute concentrations of CH_4 in TOMCAT simulations match aircraft data very well, although given the global mean surface concentration scaling we expect the magnitude of CH_4 to be well simulated. The latitudinal and vertical distributions are also well captured, giving confidence in the model transport and OH simulation."

L191-192: It looks like the model O_3 is a factor or two too low compared with aircraft observations over southern Africa and off the coast over southern Atlantic. Please elaborate on the possible reasons for this bias.

Author response: We thank the reviewer for highlighting this. Following this comment we have reassessed the comparison of simulated O_3 with the aircraft data, and extended the evaluation of O_3 using ozone sondes (Fig 1). The limited temporal coverage of the aircraft data means that we were comparing long-term mean simulated concentrations with patchy observational data. While for other species (CO, CH4 and PAN) this is the only option to carry out basic evaluation of the model and compare broad characteristics, for O_3 the OMI satellite retrievals and ozone sonde climatologies from Tilmes et al. (2012) provide a much better, more fair evaluation. The ozone sonde climatologies are long-term mean concentrations over a period directly comparable to our observations (1995-2011), therefore offering a more reliable comparison.
We therefore decided to remove the O_3 comparison with the aircraft data and conduct instead a more thorough evaluation of tropospheric O_3 against the ozone sonde climatology. We have now included a new figure in the manuscript (Fig. 1), illustrating this comparison. We believe the O_3 evaluation with both ozone sondes and satellite data provides a good

indication of the model's skill at simulating tropospheric O_3. For the other species where we present no alternative comparisons, we retain the aircraft comparisons (now Fig. 2), but have pointed out explicitly the caveats associated with these comparisons.

Changes in manuscript:
L208-211 "While the comparison of observational data from intermittent aircraft campaigns does not offer a perfect comparison with the model simulated long-term mean concentrations, it allows evaluation of broad characteristics of a number of species over vertical profiles in many global regions."

L195-196: It would be helpful to have a quantitative estimate (e.g., bias, error, correlation) of how well the model captures the observations.

Authors' response: We agree that is important to be more quantitative here. We have now calculated normalised mean biases of simulated tropospheric O_3 against ozone sonde observations from Tilmes et al. (2012). This is now included in the text as Figure 1, with discussion of the calculated bias at the beginning of section 3.

Changes in manuscript:
L190-194
"TOMCAT O_3 has also been evaluated using sonde observations (Fig. 1 and S4) (Tilmes et al., 2012), with TOMCAT generally representing the vertical profiles, seasonal variation and absolute concentrations of O_3 very well, with a normalised mean bias (NMB) of 1.1% across all sites at 700-1000 hPa and 2.1% at 300-700 hPa. The model capably simulates seasonality of tropospheric O_3 (Fig. 1), with a maximum seasonal bias of 6.3% at 300-700 hPa in March-May."

We have also calculated normalised mean biases against the aircraft observations for CH_4, CO and PAN. This figure is now included in the supplementary material (Fig. S6). We have also mentioned specific bias values in the discussion in section 3.1.

Changes in manuscript:
L217-227
CO concentrations decrease with altitude but the largest values still occur around urban areas and burning regions, which can be seen in both model and aircraft concentrations. Consistent with the comparison with MOPITT satellite retrievals (Fig. S1 and S2), the model underestimates CO concentrations particularly near the surface, with a NMB of -11.1%, -9.93% and -0.25% at 0-2 km, 2-6 km and 6-10 km, respectively. Absolute concentrations of CH_4 in TOMCAT simulations match aircraft data very well, although given the global mean surface concentration scaling we expect the magnitude of CH_4 to be well simulated. The latitudinal and vertical distributions are also well captured, giving confidence in the model transport and OH simulation. Aircraft observations show CH_4 also decreases with altitude and the hemispherical disparity becomes more pronounced, with higher concentrations in the NH. For PAN concentrations, the simulated spatial distribution is broadly well captured, as is the increased concentration with altitude. There is a general low bias in absolute concentrations near the surface (NMB=-12.3%), with better comparison at 2-6 km (NMB=1.68%) and over-estimation at 6-10 km (NMB=18.17%)."

L196-197: By how much are the simulated concentrations of NOx lower than the observations? What processes (emissions, chemistry or meteorology) are likely responsible for these biases? Do these biases in NOx have implications for the simulation of ozone?

Authors' response: The low NO_x values we simulate in TOMCAT relative to observations are very likely a result of the lower temporal and spatial resolution of the model output compared with the spatial scale on which strong gradients in NO_x are observed. The short

atmospheric lifetime of NO_x makes it difficult to compare aircraft measurements to modelled values (Huijnen et al., 2010). Underestimation of NO_x concentrations would affect tropospheric O_3, decreasing O_3 concentrations in non-urban locations and potentially causing the slight low bias in O_3 in the model. However, in this study we have conducted a thorough evaluation of tropospheric O_3 which gives us confidence that the model capably simulates O_3. We therefore decided that a direct evaluation of NO_x in TOMCAT did not add much to our analysis and it was removed from the main manuscript and replaced with an evaluation for peroxyacetyl nitrate (PAN) (Fig 2j-l). The relatively long-lived lifetime of PAN means it is a reservoir species with a less heterogeneous distribution, therefore this comparison gives a better indication of model transport and chemistry performance (Huijnen et al., 2010).

Changes in manuscript:
L223-227
"For PAN concentrations, the simulated spatial distribution is broadly well captured, as is the increased concentration with altitude. There is a general low bias in absolute concentrations near the surface (NMB=-12.3%), with better comparison at 2-6 km (NMB=1.68%) and over-estimation at 6-10 km (NMB=18.17%). "

Section 3.2: It would be useful to clarify that the OH evaluation is performed for year 2000. How is the tropopause determined to calculate tropospheric OH concentrations? How does the model tropospheric methane lifetime (due to OH reaction only) compare against that derived from observational estimates by Prather et al. (2012)?

Authors' response: The tropopause in our study was a climatological tropopause calculated from the method in Lawrence et al. (2001), using the formula:

$$\rho_{cli} = 300 - 215(\cos(\phi))^2$$

Where ϕ is latitude and ρ is pressure. We have revised the text to clarify this and also mentioned the year which was used for the evaluation:

Changes in manuscript:
L230-232
"Here we follow the evaluation methodology recommended by Lawrence et al. (2001) of dividing tropospheric OH into 12 sub-domains, from the surface to a climatologically derived tropopause. This method was also used to evaluate a previous version of TOMCAT(vn1.76) by Monks et al. (2017) allowing direct comparison. The evaluation is performed for the year 2000."

The tropospheric methane lifetime in Prather et al. (2012) is 11.2 ± 1.3 years. The lifetime from TOMCAT is below this range, however the lifetime calculated here is comparable to other model estimates in Naik et al. (2013). In addition, the distribution of OH in TOMCAT can explain the slightly lower lifetime. Mean tropospheric OH in TOMCAT fits well with other estimates (Prinn et al., 2001; Wang et al., 2008), but the OH evaluation in section 3.2 indicates that in TOMCAT OH concentrations are larger in the lower troposphere than other estimates, especially in the NH. This is also the region where methane concentrations are highest, thereby increasing the sink and decreasing the chemical methane lifetime in TOMCAT relative to other studies.

L215-216: What caused the lowering of OH in this version of TOMCAT versus that described by Monks et al (2017)?

Authors' response: The main development of TOMCAT-GLOMAP since Monks et al. (2017) is the introduction of improved cloud fields based on reanalyses, replacing the previously used climatologies. This leads to photolysis rate changes which then affect OH concentrations. We now add the following in the manuscript:

Changes in manuscript:
L244-246
"This is primarily due to an updated treatment of clouds, in which climatological cloud fields have been replaced with cloud fraction from ECMWF reanalyses data, affecting photolysis rates."

L218-219: As I understand, the authors choose to calculate the chemical lifetime rather than the atmospheric lifetime of methane from the model because not all loss processes affecting the atmospheric lifetime are considered in the model (e.g., soil uptake, stratospheric loss, tropospheric loss due to chlorine). And not "Due to the long lifetime of CH4". Please rephrase this sentence.

Authors' response: We agree that this point needs clarification. The reason for the calculation of the chemical lifetime was a combination of simplified treatment of methane in the model (i.e. the scaling) and its relatively long lifetime. Furthermore, given the focus of the paper on OH and atmospheric chemistry changes, the chemical lifetime was the most relevant measure. We have now amended the text as follows:

Changes in manuscript:
L247-250
"Due to the simplified treatment of CH_4, the scaling applied and its relatively long atmospheric lifetime, the total atmospheric lifetime cannot be determined from TOMCAT simulations. Instead a chemical lifetime due to reaction with OH is calculated from CH_4 and OH burdens, disregarding stratospheric and soil sinks (Fuglestvedt et al., 1999; Berntsen et al., 2005; Voulgarakis et al., 2013)."

L246-247: I think this sentence should be placed before describing the Voulgarakis et al (2015) results.

Authors' response: Thank you for this suggestion. This has now been reworded and moved as suggested.

Changes in manuscript:
L281-284
"Conversely, a study by Monks et al. (2012) considered CO IAV in the Arctic, finding that biomass burning was the dominant driver with a strong correlation to El Niño. Voulgarakis et al. (2015) also suggested that biomass burning was the more important driver of IAV with only a small effect from meteorology."

L250-252: Is the simulated IAV in tropospheric CO concentrations driven by biomass burning emissions similar to the IAV in the imposed biomass burning emissions? I would imagine that the IAV in GFED4 CO emissions would be similar to that for CO simulated by the model. Would be useful to confirm this. This then begs the question - what is driving the interannual variability in biomass burning emissions - is it changes in area burnt, biomass available for burning, or meteorological conditions or all of these?

Authors' response: Simulated CO IAV is slightly smaller than the IAV of biomass burning emissions from GFEDv4, with a coefficient of variation of 14.3% compared to 20.6%. This indicates a strong dependence on biomass burning IAV but with additional elements driving

tropospheric CO concentrations which limit the control of biomass burning on IAV, such as meteorology and anthropogenic emissions.
The IAV of biomass burning emissions has been investigated in a number of studies with primary drivers including precipitation and temperature (Balzter et al., 2005). Human activity (Achard et al., 2008), ENSO (Hess et al., 2001; Page et al., 2002; van der Werf et al., 2004) and Arctic oscillation (Balzter et al., 2005) have also been proposed as important drivers.

L297-298: I find this sentence confusing - is it that including CO results in a decreasing trend in OH? Though, this is not evident from figure 6.

Authors' response: We agree this was confusing. The statement was intended to say that throughout the entire simulation, the effect of CO from fires was to decrease OH concentrations. This is evidenced by negative values for CTRL-COfix in figure 7a (previously figure 6a), indicating that OH was higher when CO emissions from fires are fixed. The text has now been amended to state this more clearly.

Changes in manuscript:
L350-352
"When CO emissions from biomass burning are fixed, OH concentrations are consistently higher than in the CTRL simulation. This indicates that high CO emissions decrease global mean tropospheric OH."

L316-317: Given that the reaction rate constant of CH4+OH is strongly sensitive to temperature, approximately 2 % K^{-1} (John et al., 2012), what is the impact of assuming constant temperature in the box model on the results discussed here?

Authors' response: The impact of assuming constant temperature or varying temperature in a one-box model is shown in McNorton et al. (2016a) (figure 1c), where the impact was found to be small although not negligible. Therefore, it was decided in this study to utilise a fixed temperature box model as varying temperature has a relatively small impact on the derived methane concentrations. This is now explained in the text.

Changes in manuscript:
L372-373
"A fixed temperature was used as varying temperature has been found to have a relatively small impact on derived CH_4 concentrations (McNorton et al., 2016a)."

L332-L333: The authors mention that they compared the early mean period (1997-2001) with the end period but Figure 7 shows the early period as 1999-2003 without the influence of El Nino. Please revise this sentence.

Authors' response: 1999-2003 is correct and this has now been corrected in the text. This was used as a more appropriate mean than 1997-2001, due to the influence of the large El Nino event.

L335: Remove "a".

Authors' response: Correction made.

L337-338: The influence of shift in ozone precursor emissions from the mid-latitudes to the tropics has been demonstrated by Zhang et al. (2016).

Thank you for this point. The spatial shift in emissions described in Zhang et al. (2016) is seen in our study by the decreasingly NO_x-limited production of O_3 in India, but otherwise is not particularly evident over this relatively short period. We have now amended the text citing Zhang et al. (2016) and mention the implications of the shift in the distribution of emissions.

Changes in manuscript:
L395-397
"This shift in the spatial distribution of O_3 precursor emissions to lower latitudes leads to increased tropospheric O_3 production proportional to total emissions (Zhang et al., 2016)."

L344: This sentence is confusing. From figure 7b, it looks like India becomes "bothlimited" towards the end of the simulation.

Authors' response: We agree. The intention was to state that India does become more "both-limited" at the end of the period, but El Niño conditions seem to inhibit this trend, maintaining the NO_x-limited regime over India. The text has now been amended to clarify this:

Changes in manuscript:
L403-404
"Over India, El Niño conditions inhibit the trend towards a "both-limited" regime, as the NO_x-limited regime dominates throughout."

L347-349: Do observations also indicate this significant alteration of the vertical distribution of tropospheric ozone? How does this interpretation of the model results compare with the analysis of Chandra et al (1998) and Ziemke and Chandra (1999)?

Authors' response: Thank you for this point. We agree that this discussion is important here. We have now included more detail on the effect of El Nino on tropospheric O_3 and comparisons to previous studies. This has been included in section 4.1.

Changes in manuscript:
L410-435
"The 1997 El Niño significantly altered the vertical distribution of O_3 in the troposphere, increasing O_3 concentrations in the NH while decreasing in the SH and tropics with an overall decrease in tropospheric O_3 of -0.82% compared to the 1997-2014 mean (Fig. 9a). In the CTRL simulation there is decreased O_3 in the tropical upper troposphere, possibly related to increased convection over the Eastern Pacific (Oman et al., 2013; Neu et al., 2014). We also simulate large increases in the mid-latitude upper troposphere of both hemispheres in the CTRL and FIREFIX simulations but not in METFIX, implying that this is produced by El Niño-associated meteorological processes which promote intrusion of stratospheric air into the troposphere. These positive anomalies were also observed in Oman et al. (2013) and Zeng and Pyle (2005), attributed to El Niño influence on circulation patterns and enhanced stratospheric-troposphere exchange.

In general, the METFIX run simulates higher O_3 concentrations in the NH than the period mean and lower concentrations in the SH (Fig. 9b). This hemispherical shift is also present in the CTRL and FIREFIX simulations but with greater negative O_3 anomalies in the SH. The simulated NH increases in the CTRL simulation correspond to other studies of the 1997 El Niño (Koumoutsaris et al., 2008), while Oman et al. (2013) similarly reported negative O_3 anomalies in the SH during El Niño. Large increases in tropospheric O_3 in the Western Pacific, Indian Ocean and Europe contribute to the increase in O_3 in the NH, despite

decreased O_3 in the Eastern Pacific (Chandra et al., 1998; Koumoutsaris et al., 2008; Oman et al., 2011).

There is an overall increase in O_3 (~2%) when meteorology was fixed to an ENSO-neutral year (i.e. 2013), meaning that meteorology during the 1997 El Niño caused a decrease in tropospheric O_3 concentrations despite large increases in O_3 in regions of the upper troposphere due to stratospheric intrusion. During the 1997 El Niño we find a 0.4% increase in global tropospheric humidity compared to the period mean. This is likely partly responsible for the general decrease in O_3 due to meteorology, as increased humidity enhances O_3 loss (Stevenson et al., 2000; Isaksen et al., 2009; Kawase et al., 2011). Changes to transport and distribution of O_3 will also impact how efficiently tropospheric O_3 is produced and lost.

The similarities between the tropospheric O_3 distribution in the CTRL and FIREFIX simulations shows that fire emissions have a relatively small impact on the global distribution of O_3, but do affect absolute values, as concentrations in the FIREFIX run are significantly lower at the tropics. This is likely because of the removal of large emissions of O_3 precursors in that latitude band when fire emissions are fixed to a non-El Niño year, as several studies have found that enhanced fires in 1997 El Niño increased tropospheric O_3 in the region (Chandra et al., 1998; Thompson et al., 2001; Doherty et al., 2006; Oman et al., 2013)."

L385-L387: These are broad-brush statements which then make it easy to question the model's ability to simulate chemical composition during El Nino years and derived interpretations. As I mentioned above, a more focused evaluation would be helpful to reveal model strengths and weaknesses building confidence in the results.

Authors' response: To address this point, we have now evaluated the model response to El Niño in section 3, as well as quantifying the model performance (Fig. 1 and S7). The text in the manuscript has now been reworded to reflect this additional analysis.

Changes in manuscript:
L455-459
"Differences between model and observations may be due to a number of factors, such as the relatively coarse model resolution, uncertainties in the model emission inventories and errors in the observations. However, good overall agreement of the model with different observations, including the ability of the model to simulate the observed atmospheric responses to El Niño events (i.e. OEI change of 2.8 DU compared to 2.4 DU in Ziemke et al. (2010)) provides confidence in model performance and results."

Responses to reviewer #2:

General comment: The manuscript “Impact of El Niño Southern Oscillation on the interannual variability of methane and tropospheric ozone” written by Matthew J. Rowlinson describes the impact of meteorological variability and forest fires associated with El Niño Southern Oscillation (ENSO) on methane and tropospheric ozone. The manuscript contains novel investigation to quantitatively isolate the impact of forest fire emissions and meteorological variability on methane lifetime and growth rate using modelling approach. While many modelling studies on the impact of ENSO on tropospheric ozone have been conducted, this is an interesting work that deduced spatial variations in radiative effects of tropospheric ozone changes during El Niño. The authors used appropriate model simulations to use for this science problem. Overall this manuscript is well written and easy to follow. I would like to consider the publication of this manuscript from Atmospheric Chemistry and Physics after minor revision. Please see the following comments.

Authors’ response: We would like to thank the review for their general comments on the manuscript, suggestions for improvement and positive remarks on the study. We have endeavoured to address all specific comments and our responses and corrections are detailed below.

Specific comments:

1. Model evaluation

In Section 3, the authors presented the model evaluation of mean concentration fields of O3, CO, CH4, and NOx with satellite, aircraft, and ozonesonde observations, whereas the authors do not conduct model evaluation of inter-annual variations in these concentration fields during El Niño. The model evaluation would also be helpful to support validity of the model simulations used in this study.

Authors’ response: We agree that this is an important point which was also raised by Reviewer #1. We now clarify in section 2.1 that our model is driven by ECMWF-reanalysis, which has previously been shown to be able to represent ENSO events.

Changes in manuscript:
L133-135
“ECMWF ERA-Interim reanalyses have been shown to have good skill in capturing Madden-Julian Oscillation (MJO) events which in turn impact the onset of ENSO events (Dee et al., 2011), giving confidence that the model competently represents El Niño meteorological conditions.”

We have also compared simulated tropospheric O_3 response to El Niño events against observed responses in literature. We find that the Ozone ENSO Index (OED) from Ziemke et al. (2010) yields a response of +2.8 DU in the model compared to a +2.4 DU response in observations. We have also added a figure (Fig. S4) to the supplementary showing regional response in total O_3 column and compared this to findings of (Zhang et al., 2015). We have consequently changed the manuscript text in section 3:

Changes in manuscript:
L197-204
“We have also assessed the capability of TOMCAT-GLOMAP to simulate observed responses to El Niño events. Ziemke et al. (2010) derived an O_3 ENSO index using satellite observations, finding that for a +1K change in the Nino 3.4 index, there was a 2.4 DU increase in the OEI. In TOMCAT-GLOMAP, we calculate a 2.8 DU increase per +1K in the

Nino 3.4, indicating a slightly larger but comparable response to El Niño events. The regional response of tropospheric O_3 to El Niño was evaluated against an analysis using various observations and a chemistry-climate model in Zhang et al. (2015). The study observed increased total O_3 column in the North Pacific, southern USA, north-eastern Africa and East Asia, with decreases over central Europe and the North Atlantic. All of these observed responses were present in TOMCAT-GLOMAP simulations, except with a slight increase in central Europe and a simulated decrease in TOC in Western Europe and East Atlantic (Fig. S5). “

2. Impact of ENSO on OH and methane

In Section 4.2, the authors quantified the impact of forest fire emissions on CH4 growth rate; however, the authors do not compare it with the observed CH4 growth rate, even though the authors concluded that “This effect, combined with concurrent direct CH4 emission from fires explain the observed changes to CH4 growth rate during the 1997 El Niño” (P. 15, L. 391-392) in Section 6. I would like to recommend to add the comparison of the observed and simulated CH4 growth rate in Section 4.2. The authors also presented the impacts of forest fire emissions and meteorological variability on OH concentrations in Figure 6. Although the impacts are comparable except during the 1997-1998 El Niño, the authors hardly mentioned the impact of meteorology. A more detailed analysis (e.g., how do specific humidity, cloud, and lightning NOx affect inter-annual variations in OH?) would also be interesting, though this may be beyond the scope of the current manuscript.

Authors’ response: We thank the reviewer for this very good point and useful recommendations. Our main reason for using the box model was to analyse the effect of modelled changes to OH under different scenarios. Therefore, in our study, the difference in the changes to methane concentrations and growth rates between different simulations are more relevant than comparing the absolute methane concentrations to observed values. It is important to note that the box model only takes into account changes to CH_4 due to loss by OH, whereas observed changes are impacted by all sink and source variabilities, making the comparison difficult to make.
However, we have now also compared the simulated methane growth rate from the box model with the observed growth rate (figure 1 below). We find that in general the box model reproduces the broad trend in growth rates in the early part of the period, and in particular picks up the large change in 1998, caused by the El Niño event analysed in this study. Later in the modelled period the comparison with the observed growth rate becomes poorer.

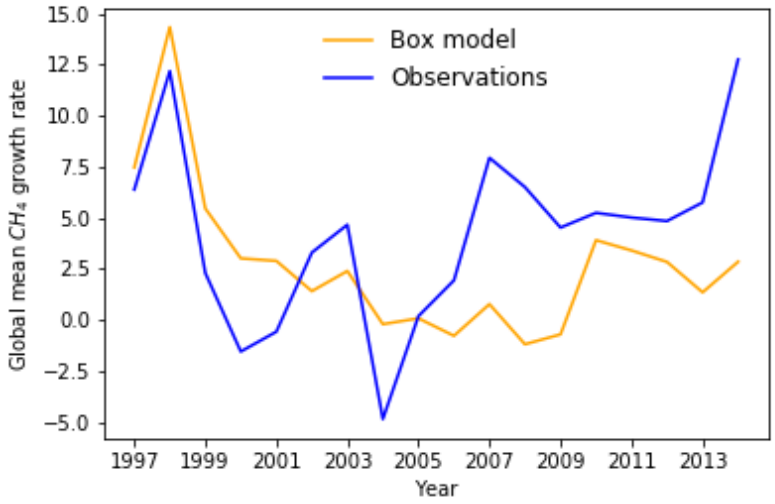

Figure 1. Comparison of global mean CH_4 concentration growth rate from the box model to the (Dlugokencky, 2019) observed values.

Regarding OH variability due to meteorology, we have now added to our discussion to consider the causes of this. Various studies have found that meteorology is important for OH variability. Nicely et al. (2018) quantified the impact of stratospheric O_3, tropospheric H_2O_2 and NO_x, temperature and circulation changes on global OH, with H_2O_2 and NO_x changes being the most important. Lightning NO_x has been found to be important for OH in Turner et al. (2018), while Murray et al. (2014) examined variability on longer timescales, finding multiple meteorological drivers.

We have now modified the manuscript as follows:

Changes in manuscript:
L324-338
"Various meteorological variables are known to affect OH and O_3 variability, including humidity, clouds and temperature (Stevenson et al., 2005; Holmes et al., 2013; Nicely et al., 2018). OH variability is particularly sensitive to changes in lightning NO_x production which decreases during El Niño conditions (Turner et al., 2018). Murray et al. (2014) also examined factors affecting OH variability since the last glacial maximum, finding tropospheric water vapour, overhead stratospheric O_3 and lightning NO_x to be key controlling factors. Furthermore, circulation changes during El Niño events have been linked to lower stratospheric O_3 variability (Zhang et al., 2015; Manatsa and Mukwada, 2017), which in turn influences tropospheric OH and O_3 concentrations (Holmes et al., 2013; Murray et al., 2014). Despite the importance of meteorological drivers, we find that fire emissions are the dominant cause of variation in both OH and O_3 during the 1997 El Niño, increasing global tropospheric O_3 burden by up to ~7% and decreasing tropospheric OH by up to ~6%. This result is supported by several other studies, which have found that during large fire events such as that caused by the 1997 El Niño, fire emissions substantially decrease tropospheric OH and increase tropospheric O_3 (Hauglustaine et al., 1999; Sudo and Takahashi, 2001; Holmes et al., 2013). Our results indicate that while meteorology is generally the most important driver of IAV in global tropospheric OH and O_3, fire emissions can also play a key role and become the dominant driver when there are particularly large fire emissions related to El Niño. "

P. 2, L. 57: Tropospheric O3 changes related to meteorology were attributed by both transport and O3 loss with water vapour in Section 4.3; why do the authors mention only atmospheric transport changes in abstract?

Authors' response: Thank you for pointing this out. We have now modified this sentence in the abstract to better account for the likely pathways of decreased tropospheric O_3 during El Niño.

Changes in manuscript:
L58-59

"El Niño-related changes in atmospheric transport and humidity decrease global tropospheric O_3 concentrations leading to a -0.03 Wm^{-2} change in the O_3 radiative effect (RE). "

P. 4, L. 139-140: Why is CH4 concentrations scaled to the observations even though the CH4 emission inventory is used in the model?

Authors' response: We agree this requires clarification. The scaling in TOMCAT applies only to the global mean surface methane, meaning that the distribution of methane, which is simulated in the model, still needs to be based on an emissions inventory. An improved explanation of the CH_4 scaling applied in TOMCAT is now included in section 2.

Changes in manuscript:
L146-148
"Global mean surface CH_4 mixing ratio is scaled in TOMCAT-GLOMAP to a best-estimate based on observed global surface mean concentration (McNorton et al., 2016a; Dlugokencky, 2019)."

P. 8, L. 242-243: What is definition of El Niño periods used in this study? Please clarify the definition.

Authors' response: El Nino periods were defined to be times when the bimonthly multivariate ENSO index was greater than 1. We have now included this important clarification in section 2.3.

Changes in manuscript:
L166
"Throughout this study, an El Niño event was taken to be ongoing if the bimonthly MEI was greater than +1.0."

P. 8, L. 253-255: I would like to recommend to add the percentage number of the increase during the 2002/2003, 2006, and 2009/2010 El Niño events to compare them with the extreme El Niño event in 1997/1998 quantitatively.

Authors' response: Thank you for this point - we agree that this more quantitative statement provides a clearer picture. We have now added these values and amended the text.

Changes in manuscript:
L289-291

"Smaller increases of 5.8% and 7.6% occur during less extreme El Niño events of 2002/2003 and 2006, respectively, with only a 1.8% increase during the 2009/2010 El Niño, indicating that El Niño only significantly impacts CO concentrations when there is an associated increase in global fire events."

P. 9, L. 271-272: Why does fire emissions have small impact on CO IAV?

Authors' response: In specific regions and seasons meteorology can be more important due to increased convective transport, but in general we report that fire emissions have a large effect on IAV.
This specific sentence stated that meteorology was more important in Africa (Sep-Oct) and Indonesia (Mar-Apr). We go on to say that these results have also been found in other studies. We have now added the following to the text to clarify possible reasons for the stronger meteorological effect on specific regions and seasons.

Changes in manuscript:
L312-315
"This is in good agreement with Voulgarakis et al. (2015) who found that with fixed biomass burning emissions there remained high IAV over Africa during Dec-Jan, and Huang et al. (2014) who found CO over Central Africa correlated more closely with ice water content than CO emissions due to increased convective transport"

P. 11, L. 300-302: Do you have possible explanation of the difference between this study and Butler et al. (2005)? Did you compare increases in CO emissions in GFED4 with Butler et al. (2005)?

Authors' response: We agree this discrepancy needed further clarification. The 9% figure given in our manuscript was a maximum monthly OH perturbation. When we average our results over the same period as Butler et al. (2005), we find a mean perturbation of -3.6%. While still slightly larger, this is much closer to the -2.2% value reported in Butler et al. (2005) and also compares well to modelled OH change due to the 1997 Indonesian wildfires in Duncan et al. (2003), of between -2.1% and -6.8%. We have amended the text in section 4.2.

Changes in manuscript:
L352-356
"The greatest impact is during the 1997 El Niño where CO emissions were abnormally large, suppressing mass weighted global monthly mean OH concentrations by up to 9%. The mean effect on OH over the 1997 El Niño of -3.6% is comparable to that simulated by Butler et al. (2005), who also found an increase in CO resulted in achange in OH of -2.2%. Duncan et al. (2003) found a similar magnitude response in OH to the Indonesian wildfires in 1997, of between -2.1% and -6.8%."

P. 13, L. 327: Please clarify the reason why you conducted this analysis in Section 4.3.

Authors' response: We have now included justification for this analysis at the start of section 4.3.

Changes in manuscript:
L382-384
"In this section we examine trends and the impact of El Niño on the production of tropospheric O_3. El Niño is known to have large effects on tropospheric O_3 precursors such as CO and NO_x, therefore examining O_3 production regimes during El Nino can provide insights into the main mechanism responsible for the observed changes in tropospheric O_3."

P. 14, L. 346-362: Many previous works have been done with different models and satellite observations with regard to ENSO impacts on tropospheric ozone. It would be beneficial to see more discussion of how the results presented here compare to previous studies (e.g., Stevenson et al., 2005; Zeng and Pyle, 2005; Doherty et al., 2006; Koumoutsaris et al., 2008; Nassar et al., 2009; Ziemke et al., 2010; Sekiya and Sudo, 2012; Oman et al., 2013; Neu et al., 2014; Inness et al., 2015).

Authors' response: Thank you for this point. We agree that the limited discussion of El Nino and tropospheric O_3 was a weakness of the original manuscript. We have now added substantially enhanced this discussion, including comparison to observations and previous studies, clarifying how our findings relate and offering improved explanations for the changes in our simulations.

Changes in manuscript:
L410-435
The 1997 El Niño significantly altered the vertical distribution of O_3 in the troposphere, increasing O_3 concentrations in the NH while decreasing in the SH and tropics with an overall decrease in tropospheric O_3 of -0.82% compared to the 1997-2014 mean (Fig. 9a). In the CTRL simulation there is decreased O_3 in the tropical upper troposphere, possibly related to increased convection over the Eastern Pacific (Oman et al., 2013; Neu et al., 2014). We also simulate large increases in the mid-latitude upper troposphere of both hemispheres in the CTRL and FIREFIX simulations but not in METFIX, implying that this is produced by El Niño-associated meteorological processes which promote intrusion of stratospheric air into the troposphere. These positive anomalies were also observed in Oman et al. (2013) and Zeng and Pyle (2005), attributed to El Niño influence on circulation patterns and enhanced stratospheric-troposphere exchange.

In general, the METFIX run simulates higher O_3 concentrations in the NH than the period mean and lower concentrations in the SH (Fig. 9b). This hemispherical shift is also present in the CTRL and FIREFIX simulations but with greater negative O_3 anomalies in the SH. The simulated NH increases in the CTRL simulation correspond to other studies of the 1997 El Niño (Koumoutsaris et al., 2008), while Oman et al. (2013) similarly reported negative O_3 anomalies in the SH during El Niño. Large increases in tropospheric O_3 in the Western Pacific, Indian Ocean and Europe contribute to the increase in O_3 in the NH, despite decreased O_3 in the Eastern Pacific (Chandra et al., 1998; Koumoutsaris et al., 2008; Oman et al., 2011).

There is an overall increase in O_3 (~2%) when meteorology was fixed to an ENSO-neutral year (i.e. 2013), meaning that meteorology during the 1997 El Niño caused a decrease in tropospheric O_3 concentrations despite large increases in O_3 in regions of the upper troposphere due to stratospheric intrusion. During the 1997 El Niño we find a 0.4% increase in global tropospheric humidity compared to the period mean. This is likely partly responsible for the general decrease in O_3 due to meteorology, as increased humidity enhances O_3 loss (Stevenson et al., 2000; Isaksen et al., 2009; Kawase et al., 2011). Changes to transport and distribution of O_3 will also impact how efficiently tropospheric O_3 is produced and lost.

The similarities between the tropospheric O_3 distribution in the CTRL and FIREFIX simulations show that fire emissions have a relatively small impact on the global distribution of O_3, but do affect absolute values, as concentrations in the FIREFIX run are significantly lower at the tropics. This is likely because of the removal of large emissions of O_3 precursors in that latitude band when fire emissions are fixed to a non-El Niño year, as several studies

have found that enhanced fires in 1997 El Niño increased tropospheric O_3 in the region (Chandra et al., 1998; Thompson et al., 2001; Doherty et al., 2006; Oman et al., 2013)."

P. 14, L. 364-365: Do the authors used TES O3 radiative kernel? Please clarify what data the authors used in this study.

Authors' response: We agree that more clarity is needed here. We used the tropospheric O_3 radiative kernel produced by Rap et al. (2015) using the Edwards-Slingo offline radiative transfer model. We have amended the text in section 2.2 to make this clear.

Changes in manuscript:
L150-151
"Radiative effects of O_3 changes are calculated using the O_3 radiative kernel approach derived by Rap et al. (2015) using an offline version of the Edwards and Slingo (1996) radiative transfer model."

Technical corrections:

P. 2. L. 58: typo for nitrogen oxides?

Authors' response: Thank you for pointing this. Correction made.

P. 4, L. 135: typo for nitrogen oxides?

Authors' response: Correction made.

P. 13, L. 332: Which is correct, "1997-2001" or "1999-2003"? The "1999-2003" period would be appropriate to obtain the mean fields.

Authors' response: Thank you for pointing this. 1999-2003 is correct and this has now been corrected in the text. This was used as a more appropriate mean than 1997-2001, due to the influence of the large El Nino event.

Changes in manuscript:
L390-391
"We compare the early period mean (1999-2003) to the end period mean (2010-2014) to determine whether significant changes have occurred over the 18-year period, and compared mean El Niño conditions to both."

References

Achard, F., Eva, H. D., Mollicone, D., and Beuchle, R.: The effect of climate anomalies and human ignition factor on wildfires in Russian boreal forests, 363, 2329-2337, doi:10.1098/rstb.2007.2203, 2008.

Balzter, H., Gerard, F. F., George, C. T., Rowland, C. S., Jupp, T. E., McCallum, I., Shvidenko, A., Nilsson, S., Sukhinin, A., Onuchin, A., and Schmullius, C.: Impact of the Arctic Oscillation pattern on interannual forest fire variability in Central Siberia, 32, 10.1029/2005gl022526, 2005.

Berntsen, T. K., Fuglestvedt, J. S., Joshi, M. M., Shine, K. P., Stuber, N., Ponater, M., Sausen, R., Hauglustaine, D. A., and Li, L.: Response of climate to regional emissions of ozone precursors: sensitivities and warming potentials, Tellus B: Chemical and Physical Meteorology, 57, 283-304, 10.3402/tellusb.v57i4.16549, 2005.

Butler, T. M., Rayner, P. J., Simmonds, I., and Lawrence, M. G.: Simultaneous mass balance inverse modeling of methane and carbon monoxide, Journal of Geophysical Research: Atmospheres, 110, doi:10.1029/2005JD006071, 2005.

Chandra, S., Ziemke, J. R., Min, W., and Read, W. G.: Effects of 1997–1998 El Niño on tropospheric ozone and water vapor, Geophysical Research Letters, 25, 3867-3870, 10.1029/98GL02695, 1998.

Dee, D. P., Uppala, S. M., Simmons, A. J., Berrisford, P., Poli, P., Kobayashi, S., Andrae, U., Balmaseda, M. A., Balsamo, G., Bauer, P., Bechtold, P., Beljaars, A. C. M., van de Berg, L., Bidlot, J., Bormann, N., Delsol, C., Dragani, R., Fuentes, M., Geer, A. J., Haimberger, L., Healy, S. B., Hersbach, H., Hólm, E. V., Isaksen, L., Kållberg, P., Köhler, M., Matricardi, M., McNally, A. P., Monge-Sanz, B. M., Morcrette, J.-J., Park, B.-K., Peubey, C., de Rosnay, P., Tavolato, C., Thépaut, J.-N., and Vitart, F.: The ERA-Interim reanalysis: configuration and performance of the data assimilation system, 137, 553-597, 10.1002/qj.828, 2011.

Dlugokencky, E.: NOAA/ESRL, (www.esrl.noaa.gov/gmd/ccgg/trends_ch4/), 2019.

Doherty, R. M., Stevenson, D. S., Johnson, C. E., Collins, W. J., and Sanderson, M. G.: Tropospheric ozone and El Niño–Southern Oscillation: Influence of atmospheric dynamics, biomass burning emissions, and future climate change, 111, 10.1029/2005jd006849, 2006.

Duncan, B. N., Bey, I., Chin, M., Mickley, L. J., Fairlie, T. D., Martin, R. V., and Matsueda, H.: Indonesian wildfires of 1997: Impact on tropospheric chemistry, 108, 10.1029/2002jd003195, 2003.

Duncan, B. N., Logan, J. A., Bey, I., Megretskaia, I. A., Yantosca, R. M., Novelli, P. C., Jones, N. B., and Rinsland, C. P.: Global budget of CO, 1988–1997: Source estimates and validation with a global model, 112, 10.1029/2007jd008459, 2007.

Emmons, L. K., Deeter, M. N., Gille, J. C., Edwards, D. P., Attié, J.-L., Warner, J., Ziskin, D., Francis, G., Khattatov, B., Yudin, V., Lamarque, J.-F., Ho, S.-P., Mao, D., Chen, J. S., Drummond, J., Novelli, P., Sachse, G., Coffey, M. T., Hannigan, J. W., Gerbig, C., Kawakami, S., Kondo, Y., Takegawa, N., Schlager, H., Baehr, J., and Ziereis, H.: Validation of Measurements of Pollution in the Troposphere (MOPITT) CO retrievals with aircraft in situ profiles, Journal of Geophysical Research: Atmospheres, 109, doi:10.1029/2003JD004101, 2004.

Fuglestvedt, J. S., Berntsen, T. K., Isaksen, I. S. A., Mao, H., Liang, X.-Z., and Wang, W.-C.: Climatic forcing of nitrogen oxides through changes in tropospheric ozone and methane; global 3D model studies, Atmospheric Environment, 33, 961-977, https://doi.org/10.1016/S1352-2310(98)00217-9, 1999.

Hauglustaine, D. A., Brasseur, G. P., and Levine, J. S.: A sensitivity simulation of tropospheric ozone changes due to the 1997 Indonesian fire emissions, 26, 3305-3308, 10.1029/1999gl900610, 1999.

Hess, J. C., Scott, C. A., Hufford, G. L., and Fleming, M. D.: El Niño and its impact on fire weather conditions in Alaska, International Journal of Wildland Fire, 10, 1-13, 10.1071/WF01007, 2001.

Holmes, C. D., Prather, M. J., Søvde, O. A., and Myhre, G.: Future methane, hydroxyl, and their uncertainties: key climate and emission parameters for future predictions, Atmos. Chem. Phys., 13, 285-302, 10.5194/acp-13-285-2013, 2013.

Huang, L., Fu, R., and Jiang, J. H.: Impacts of fire emissions and transport pathways on the interannual variation of CO in the tropical upper troposphere, Atmos. Chem. Phys., 14, 4087-4099, 10.5194/acp-14-4087-2014, 2014.

Huijnen, V., Eskes, H. J., Poupkou, A., Elbern, H., Boersma, K. F., Foret, G., Sofiev, M., Valdebenito, A., Flemming, J., Stein, O., Gross, A., Robertson, L., D'Isidoro, M., Kioutsioukis, I., Friese, E., Amstrup, B., Bergstrom, R., Strunk, A., Vira, J., Zyryanov, D., Maurizi, A., Melas, D., Peuch, V. H., and Zerefos, C.: Comparison of OMI NO₂ tropospheric columns with an ensemble of global and European regional air quality models, Atmos. Chem. Phys., 10, 3273-3296, 10.5194/acp-10-3273-2010, 2010.

Isaksen, I. S. A., Granier, C., Myhre, G., Berntsen, T. K., Dalsøren, S. B., Gauss, M., Klimont, Z., Benestad, R., Bousquet, P., Collins, W., Cox, T., Eyring, V., Fowler, D., Fuzzi, S., Jöckel, P., Laj, P., Lohmann, U., Maione, M., Monks, P., Prevot, A. S. H., Raes, F., Richter, A., Rognerud, B., Schulz, M., Shindell, D., Stevenson, D. S., Storelvmo, T., Wang, W. C., van Weele, M., Wild, M., and Wuebbles, D.: Atmospheric composition change: Climate–Chemistry interactions, Atmospheric Environment, 43, 5138-5192, https://doi.org/10.1016/j.atmosenv.2009.08.003, 2009.

Kawase, H., Nagashima, T., Sudo, K., and Nozawa, T.: Future changes in tropospheric ozone under Representative Concentration Pathways (RCPs), 38, doi:10.1029/2010GL046402, 2011.

Koumoutsaris, S., Bey, I., Generoso, S., and Thouret, V.: Influence of El Niño–Southern Oscillation on the interannual variability of tropospheric ozone in the northern midlatitudes, Journal of Geophysical Research: Atmospheres (1984–2012), 113, 10.1029/2007JD009753, 2008.

Lathière, J., Hauglustaine, D. A., De Noblet-Ducoudré, N., Krinner, G., and Folberth, G. A.: Past and future changes in biogenic volatile organic compound emissions simulated with a global dynamic vegetation model, 32, 10.1029/2005gl024164, 2005.

Lawrence, M., Jöckel, P., and Kuhlmann, R.: What does the global mean OH concentration tell us?, 2001.

Manatsa, D., and Mukwada, G.: A connection from stratospheric ozone to El Niño-Southern Oscillation, Scientific Reports, 7, 5558, 10.1038/s41598-017-05111-8, 2017.

Matthews, E., and Fung, I.: Methane emission from natural wetlands: Global distribution, area, and environmental characteristics of sources, 1, 61-86, 10.1029/GB001i001p00061, 1987.

McNorton, J., Chipperfield, M., Gloor, M., Wilson, C., Wuhu, F., Hayman, G., Rigby, M., B. Krummel, P., O'Doherty, S., Prinn, R., Weiss, R., Young, D., Dlugokencky, E., and Montzka, S. A.: Role of OH variability in the stalling of the global atmospheric CH4 growth rate from 1999 to 2006, 1-24 pp., 2016a.

McNorton, J., Gloor, E., Wilson, C., Hayman, G. D., Gedney, N., Comyn-Platt, E., Marthews, T., Parker, R. J., Boesch, H., and Chipperfield, M. P.: Role of regional wetland emissions in atmospheric methane variability, 43, 11,433-411,444, 10.1002/2016gl070649, 2016b.

Monks, S., R. Arnold, S., Hollaway, M., Pope, R., Wilson, C., Wuhu, F., Emmerson, K., J. Kerridge, B., Latter, B., M. Miles, G., Siddans, R., and P. Chipperfield, M.: The TOMCAT global chemical transport model v1.6: Description of chemical mechanism and model evaluation, 3025-3057 pp., 2017.

Monks, S. A., Arnold, S. R., and Chipperfield, M. P.: Evidence for El Niño–Southern Oscillation (ENSO) influence on Arctic CO interannual variability through biomass burning emissions, Geophysical Research Letters, 39, doi:10.1029/2012GL052512, 2012.

Murray, L. T., Mickley, L. J., Kaplan, J. O., Sofen, E. D., Pfeiffer, M., and Alexander, B.: Factors controlling variability in the oxidative capacity of the troposphere since the Last Glacial Maximum, Atmos. Chem. Phys., 14, 3589-3622, 10.5194/acp-14-3589-2014, 2014.

Naik, V., Delire, C., and Wuebbles, D. J.: Sensitivity of global biogenic isoprenoid emissions to climate variability and atmospheric CO2, 109, 10.1029/2003jd004236, 2004.

Naik, V., Voulgarakis, A., Fiore, A. M., Horowitz, L. W., Lamarque, J. F., Lin, M., Prather, M. J., Young, P. J., Bergmann, D., Cameron-Smith, P. J., Cionni, I., Collins, W. J., Dalsøren, S. B., Doherty, R., Eyring, V., Faluvegi, G., Folberth, G. A., Josse, B., Lee, Y. H., MacKenzie, I. A., Nagashima, T., van Noije, T. P. C., Plummer, D. A., Righi, M., Rumbold, S. T., Skeie, R., Shindell, D. T., Stevenson, D. S., Strode, S., Sudo, K., Szopa, S., and Zeng, G.: Preindustrial to present-day changes in tropospheric hydroxyl radical and methane lifetime from the Atmospheric Chemistry and Climate Model Intercomparison Project (ACCMIP), Atmos. Chem. Phys., 13, 5277-5298, 10.5194/acp-13-5277-2013, 2013.

Neu, J. L., Flury, T., Manney, G. L., Santee, M. L., Livesey, N. J., and Worden, J.: Tropospheric ozone variations governed by changes in stratospheric circulation, Nature Geoscience, 7, 340, 10.1038/ngeo2138

https://www.nature.com/articles/ngeo2138#supplementary-information, 2014.

Nicely, J. M., Canty, T. P., Manyin, M., Oman, L. D., Salawitch, R. J., Steenrod, S. D., Strahan, S. E., and Strode, S. A.: Changes in Global Tropospheric OH Expected as a Result of Climate Change Over the Last Several Decades, 123, 10,774-710,795, 10.1029/2018jd028388, 2018.

Oman, L. D., Ziemke, J. R., Douglass, A. R., Waugh, D. W., Lang, C., Rodriguez, J. M., and Nielsen, J. E.: The response of tropical tropospheric ozone to ENSO, 38, 10.1029/2011gl047865, 2011.

Oman, L. D., Douglass, A. R., Ziemke, J. R., Rodriguez, J. M., Waugh, D. W., and Nielsen, J. E.: The ozone response to ENSO in Aura satellite measurements and a chemistry-climate simulation, 118, 965-976, 10.1029/2012jd018546, 2013.

Page, S. E., Siegert, F., Rieley, J. O., Boehm, H.-D. V., Jaya, A., and Limin, S.: The amount of carbon released from peat and forest fires in Indonesia during 1997, Nature, 420, 61-65, 10.1038/nature01131, 2002.

Prather, M. J., Holmes, C. D., and Hsu, J.: Reactive greenhouse gas scenarios: Systematic exploration of uncertainties and the role of atmospheric chemistry, 39, 10.1029/2012gl051440, 2012.

Prinn, R. G., Huang, J., Weiss, R. F., Cunnold, D. M., Fraser, P. J., Simmonds, P. G., McCulloch, A., Harth, C., Salameh, P., O'Doherty, S., Wang, R. H. J., Porter, L., and Miller, B. R.: Evidence for Substantial Variations of Atmospheric Hydroxyl Radicals in the Past Two Decades, Science, 292, 1882-1888, 10.1126/science.1058673, 2001.

Randerson, J. T., Van Der Werf, G. R., Giglio, L., Collatz, G. J., and Kasibhatla, P. S.: Global Fire Emissions Database, Version 4.1 (GFEDv4), in, ORNL Distributed Active Archive Center, 2017.

Rap, A., Richards, N. A. D., Forster, P. M., Monks, S. A., Arnold, S. R., and Chipperfield, M. P.: Satellite constraint on the tropospheric ozone radiative effect, Geophysical Research Letters, 42, 5074-5081, doi:10.1002/2015GL064037, 2015.

Sindelarova, K., Granier, C., Bouarar, I., Guenther, A., Tilmes, S., Stavrakou, T., Müller, J. F., Kuhn, U., Stefani, P., and Knorr, W.: Global data set of biogenic VOC emissions calculated by the MEGAN model over the last 30 years, Atmos. Chem. Phys., 14, 9317-9341, 10.5194/acp-14-9317-2014, 2014.

Stevenson, D., Doherty, R., Sanderson, M., Johnson, C., Collins, B., and Derwent, D.: Impacts of climate change and variability on tropospheric ozone and its precursors, Faraday discussions, 130, 41-57; discussion 125-151, 519-124, 2005.

Stevenson, D. S., Johnson, C. E., Collins, W. J., Derwent, R. G., and Edwards, J. M.: Future estimates of tropospheric ozone radiative forcing and methane turnover — The impact of climate change, 27, 2073-2076, doi:10.1029/1999GL010887, 2000.

Sudo, K., and Takahashi, M.: Simulation of tropospheric ozone changes during 1997–1998 El Niño: Meteorological impact on tropospheric photochemistry, 28, 4091-4094, 10.1029/2001gl013335, 2001.

Thompson, A. M., Witte, J. C., Hudson, R. D., Guo, H., Herman, J. R., and Fujiwara, M.: Tropical Tropospheric Ozone and Biomass Burning, 291, 2128-2132, 10.1126/science.291.5511.2128 %J Science, 2001.

Tilmes, S., Lamarque, J. F., Emmons, L. K., Conley, A., Schultz, M. G., Saunois, M., Thouret, V., Thompson, A. M., Oltmans, S. J., Johnson, B., and Tarasick, D.: Ozonesonde climatology between 1995 and 2011: description, evaluation and applications, Atmos. Chem. Phys., 12, 7475-7497, 10.5194/acp-12-7475-2012, 2012.

Turner, A. J., Fung, I., Naik, V., Horowitz, L. W., and Cohen, R. C.: Modulation of hydroxyl variability by ENSO in the absence of external forcing, 115, 8931-8936, 10.1073/pnas.1807532115 %J Proceedings of the National Academy of Sciences, 2018.

van der Werf, G. R., Randerson, J. T., Collatz, G. J., Giglio, L., Kasibhatla, P. S., Arellano, A. F., Olsen, S. C., and Kasischke, E. S.: Continental-Scale Partitioning of Fire Emissions During the 1997 to 2001 El Niño/La Niña Period, Science, 303, 73-76, 10.1126/science.1090753, 2004.

Voulgarakis, A., Naik, V., Lamarque, J. F., Shindell, D. T., Young, P. J., Prather, M. J., Wild, O., Field, R. D., Bergmann, D., Cameron-Smith, P., Cionni, I., Collins, W. J., Dalsøren, S. B., Doherty, R. M., Eyring, V., Faluvegi, G., Folberth, G. A., Horowitz, L. W., Josse, B., MacKenzie, I. A., Nagashima, T., Plummer, D. A., Righi, M., Rumbold, S. T., Stevenson, D. S., Strode, S. A., Sudo, K., Szopa, S., and Zeng, G.: Analysis of present day and future OH and methane lifetime in the ACCMIP simulations, Atmos. Chem. Phys., 13, 2563-2587, 10.5194/acp-13-2563-2013, 2013.

Voulgarakis, A., Marlier, M. E., Faluvegi, G., Shindell, D. T., Tsigaridis, K., and Mangeon, S.: Interannual variability of tropospheric trace gases and aerosols: The role of biomass burning emissions, Journal of Geophysical Research: Atmospheres, 120, 7157-7173, doi:10.1002/2014JD022926, 2015.

Wang, J. S., McElroy, M. B., Logan, J. A., Palmer, P. I., Chameides, W. L., Wang, Y., and Megretskaia, I. A.: A quantitative assessment of uncertainties affecting estimates of global mean OH derived from methyl chloroform observations, Journal of Geophysical Research: Atmospheres, 113, doi:10.1029/2007JD008496, 2008.

Yan, X., Akiyama, H., Yagi, K., and Akimoto, H.: Global estimations of the inventory and mitigation potential of methane emissions from rice cultivation conducted using the 2006 Intergovernmental Panel on Climate Change Guidelines, 23, 10.1029/2008gb003299, 2009.

Zeng, G., and Pyle, J. A.: Influence of El Niño Southern Oscillation on stratosphere/troposphere exchange and the global tropospheric ozone budget, 32, 10.1029/2004gl021353, 2005.

Zhang, J., Tian, W., Wang, Z., Xie, F., and Wang, F.: The Influence of ENSO on Northern Midlatitude Ozone during the Winter to Spring Transition, 28, 4774-4793, 10.1175/jcli-d-14-00615.1, 2015.

Zhang, Y., Cooper, O. R., Gaudel, A., Thompson, A. M., Nédélec, P., Ogino, S.-Y., and West, J. J.: Tropospheric ozone change from 1980 to 2010 dominated by equatorward redistribution of emissions, Nature Geoscience, 9, 875, 10.1038/ngeo2827 https://www.nature.com/articles/ngeo2827#supplementary-information, 2016.

Ziemke, J. R., Chandra, S., Oman, L. D., and Bhartia, P. K.: A new ENSO index derived from satellite measurements of column ozone, Atmos. Chem. Phys., 10, 3711-3721, 10.5194/acp-10-3711-2010, 2010.

Impact of El Niño Southern Oscillation on the interannual variability of methane and tropospheric ozone

Matthew J. Rowlinson[1], Alexandru Rap[1], Stephen R. Arnold[1], Richard J. Pope[1,2], Martyn P. Chipperfield[1,2], Joe McNorton[3], Piers Forster[4], Hamish Gordon[1], Kirsty J. Pringle[1], Wuhu Feng[1,5], Brian J. Kerridge[6,7], Barry L. Latter[6,7], Richard Siddans[6,7]

[1]Institute for Climate and Atmospheric Science, School of Earth and Environment, University of Leeds, Leeds, LS2 9JT, UK
[2]National Centre for Earth Observation, University of Leeds, Leeds, LS2 9JT, UK
[3]European Centre for Medium-Range Weather Forecasts, Reading, RG2 9AX, UK
[4]Priestley International Centre for Climate, University of Leeds, LS2 9JT, Leeds, UK
[5]National Centre for Atmospheric Science, University of Leeds, LS2 9JT, Leeds, UK
[6]Remote Sensing Group, STFC Rutherford Appleton Laboratory, Harwell, Oxfordshire, UK
[7]National Centre for Earth Observation, Harwell, Oxfordshire, UK

Correspondence to: Matthew J. Rowlinson (ee11mr@leeds.ac.uk)

Abstract. ~~The growth rate of global methane (CH_4) concentrations has a strong interannual variability which is believed to be driven largely by fluctuations in CH_4 emissions from wetlands and wildfires, as well as changes to the atmospheric sink. The El Niño Southern Oscillation (ENSO) is known to influence fire occurrence, wetland emission and atmospheric transport, but there are still important uncertainties associated with the exact mechanism and magnitude of this influence.~~

The interannual variability of greenhouse gases methane (CH_4) and tropospheric ozone (O_3) is largely driven by natural variations in global emissions and meteorology. The El Niño Southern Oscillation (ENSO) is known to influence fire occurrence, wetland emission and atmospheric circulation, affecting sources and sinks of CH_4 and tropospheric O_3, but there are still important uncertainties associated with the exact mechanism and magnitude of this effect. Here we use a modelling approach to investigate how fires and meteorology control the interannual variability of global carbon monoxide (CO), CH_4 and ozone (O_3) concentrations, particularly during large El Niño events. Using a three-dimensional chemical transport model (TOMCAT) coupled to a sophisticated aerosol microphysics scheme (GLOMAP) we simulate changes to CO, hydroxyl radical (OH) and O_3 for the period 1997-2014. We then use an offline radiative transfer model to quantify the impact of changes to atmospheric composition as a result of specific drivers.

During the El Niño event of 1997-1998, there were increased emissions from biomass burning globally. As a result, global CO concentrations increased by more than 40%. This resulted in decreased global mass-weighted tropospheric OH concentrations of up to 9% and a resulting 4% increase in the CH_4 atmospheric lifetime. The change in CH_4 lifetime led to a 7.5ppb yr^{-1} increase in global mean CH_4 growth rate in 1998. Therefore biomass burning emission of CO could account for 72% of the total effect of fire emissions on CH_4 growth rate in 1998.

Our simulations indicate variations in fire emissions and meteorology associated with El Niño have opposing impacts on tropospheric O_3 burden. El Niño-related changes in atmospheric transport and humidity ~~changes~~ decrease global tropospheric O_3 concentrations leading to a -0.03 Wm^{-2} change in O_3 radiative effect (RE). However, enhanced fire emission of precursors such as nitrous oxides (NO_x) and CO increase O_3 RE by 0.03 Wm^{-2}. While globally the two mechanisms nearly cancel out, causing only a small change in global mean O_3 RE, the regional changes are large – up to -0.33 Wm^{-2} with potentially important consequences for atmospheric heating and dynamics.

1 Introduction

In terms of radiative forcing, methane (CH_4) is the second most important anthropogenically emitted greenhouse gas after CO_2 (Myhre et al., 2013). Concentrations of CH_4 have risen from approximately 722 ppb in 1750 to over 1850 ppb in 2018, an increase of more than 150% (Dlugokencky, 2019). During this time period CH_4 has contributed an estimated radiative forcing (RF) of 0.48 ± 0.05 Wm^{-2}, around 20% of the total direct anthropogenic RF from greenhouse gases (Myhre et al., 2013). Furthermore, CH_4 is a precursor of tropospheric ozone (O_3), which is also a greenhouse gas responsible for RF of 0.4 ± 0.2 Wm^{-2} since the pre-industrial (Myhre et al., 2013), as well as a harmful pollutant that damages human health (Anenberg et al., 2010) and ecosystems (Sitch et al., 2007). While anthropogenic emissions have driven the long-term increase in CH_4 concentrations, CH_4 is also emitted from a range of natural sources leading to strong interannual variability (IAV) (Bousquet et al., 2006; Dlugokencky et al., 2011; Nisbet et al., 2016). Understanding the mechanisms driving IAV is important for accurate predictions of future CH_4 concentrations, especially in the context of anthropogenic emission reductions.

Previous studies indicate that although anthropogenic sources may contribute to seasonal variations in atmospheric CH_4, natural sources are the primary drivers of IAV (Bousquet et al., 2006; Meng et al., 2015). Emissions from natural wetlands have been shown to be the dominant process, with emissions from fires and changes to the atmospheric sink also playing important roles (Bousquet et al., 2006; Chen and Prinn, 2006; Dlugokencky et al., 2011; Kirschke et al., 2013; McNorton et al., 2016a; Corbett et al., 2017). These natural sources are climate sensitive, so interannual changes to temperature and precipitation affect the amount of CH_4 emitted into the atmosphere as well as the spatial distribution (Zhu et al., 2017). Studies have found that biomass burning emissions are largely responsible for the IAV of carbon monoxide (CO) and also affect O_3 concentrations (Granier et al., 2000; Monks et al., 2012; Voulgarakis et al., 2015). Although Szopa et al. (2007) found meteorology is a more important driver of IAV for CO, explaining 50-90% of IAV.

A major driver of climatic IAV is the El Niño Southern Oscillation (ENSO) – a mode of climate variability originating in the Pacific Ocean with alternating warm (El Niño) and cold (La Niña) modes (McPhaden et al., 2006). Positive phase El Niño events lead to warmer and drier conditions in much of the tropics, disrupting global circulation patterns and leading to widespread changes in fire occurrence, wetland emissions and atmospheric transport (Feely et al., 1987; Jones et al., 2001; McPhaden et al., 2006). These influences occur most strongly in the tropics but have global consequences (Jones et al., 2001). Global CH_4 concentrations have been observed to increase significantly during El Niño events, with an especially strong signal during the 1997-1998 event when the CH_4 growth rate was 12 ppb yr^{-1}, almost triple the 1750-2018 mean annual growth rate (Rigby et al., 2008; Hodson et al., 2011). Due to the wide-ranging effects of El Niño and varied sources of CH_4, there are multiple factors which could trigger the increase in CH_4 growth rate. Chen and Prinn (2006) attributed the increase to anomalies in global wetland emissions; however Zhu et al. (2017) estimated that although 49% of the interannual variation in wetland emissions can be explained by ENSO, wetland emissions were significantly lower during El Niño including the 1997-1998 event. Bousquet et al. (2006) suggested that the increased CH_4 growth rate during the 1997-1998 El Niño was primarily caused by abnormally large peat fires in Indonesia emitting huge amounts of CH_4 while wetlands emissions remained stable (van der Werf et al., 2004; Butler et al., 2005; Bousquet et al., 2006).

In addition to direct emissions of CH_4 from fires, it has been proposed that anomalously large CO emissions during enhanced El Niño fire events could explain the changes to CH_4 growth rate (Butler et al., 2005; Bousquet et al., 2006). CO is emitted from biomass burning in much larger quantities than CH_4 (~20x larger) and its reaction with the hydroxyl radical (OH) is its primary atmospheric sink (Voulgarakis and Field, 2015). Abnormal increases in CO concentrations may suppress the availability of OH, thereby extending CH_4 lifetime and increasing its growth rate during and following large fire events (Butler et al., 2005; Manning et al., 2005). The reaction of CH_4 with OH is the largest term in the global CH_4 budget, accounting for ~90% of its sink (McNorton et al., 2016a), therefore even minor changes to OH caused by the presence of other compounds or changes to atmospheric transport and photolysis rates could have a large impact on CH_4 growth rate (Dlugokencky et al.,

2011). Butler et al. (2005) found that CO emissions suppressed OH concentrations by 2.2% in 1997-1998, which accounted for 75% of the observed change in CH_4 concentration. Bousquet et al. (2006) also reported a weakened OH sink during this El Niño event.

Here we use a modelling approach to investigate how El Niño events affect global CH_4, CO and tropospheric O_3 concentrations through changes to fire occurrence and atmospheric transport. Using long-term simulations spanning multiple El Niño and La Niña events, we quantify the relative influence of changes to fire emissions and dynamical transport. We also differentiate between the effect of direct CH_4 emissions from fires and the indirect effect via CO emissions and atmospheric chemistry changes.

2 Models and Simulations

2.1 Model description

For this study we use the TOMCAT chemical transport model (Chipperfield, 2006) coupled to the GLOMAP global aerosol microphysics scheme (Mann et al., 2010). The version of TOMCAT-GLOMAP used here is a further development of the version described by Monks et al. (2017). Cloud fields are now provided from the European Centre for Medium-Range Weather Forecasts (ECMWF) reanalyses (Dee et al., 2010), replacing the climatological clouds fields used previously from the International Satellite Cloud Climatology Project (ISCCP) (Rossow and Schiffer, 1999), leading to improved representation of photolysis. Other developments include updated emission inventories, the inclusion of CERN CLOUD-based new particle formation and the introduction of Martensson sea spray emissions (Gordon et al., 2017; Monks et al., 2017). The model is run at 2.8° x 2.8° horizontal resolution with 31 vertical levels, driven by 6-hourly ECMWF ERA-Interim reanalyses. The planetary boundary layer (PBL) scheme is based on Holtslag and Boville (1993) and sea surface temperatures are from ECMWF reanalyses. ECMWF ERA-Interim reanalyses have been shown to have good skill in capturing Madden-Julian Oscillation (MJO) events which in turn impact the onset of ENSO events (Dee et al., 2011), giving confidence that the model competently simulates El Niño meteorological conditions

The tropospheric chemistry scheme used is as described in Monks et al. (2017) with anthropogenic emissions from the Monitoring Atmospheric Composition and Climate (MACCity) emissions inventories (Lamarque et al., 2010). Annually varying emission inventories are included for all fire-emitted gas-species, aerosol emissions such as black carbon (BC) and all sources of CH_4. The Global Fire Emissions Database (GFED) used by TOMCAT-GLOMAP has been updated to version 4 with CO, nitrous oxides (NO_x) and volatile organic compound (VOC) emissions from fires (Randerson et al., 2017; Reddington et al., 2018). Monthly varying biogenic VOC emissions are from the MEGAN-MACC emissions inventory for reference year 2000, calculated from the Model of Emissions of Gases and Aerosols from Nature (MEGANv2) (Sindelarova et al., 2014). The CH_4 inventory was produced by McNorton et al. (2016b), with wetland emissions derived from the Joint UK Land Environment Simulator (JULES) and biomass burning emissions from GFEDv4 (Randerson et al., 2017). These are then combined with anthropogenic emissions from EDGARv3.2, paddy field emissions from Yan et al. (2009) and termite, wild animal, mud volcano, hydrate and ocean emissions from Matthews and Fung (1987) (McNorton et al., 2016b). The global mean surface CH_4 mixing ratio is scaled in TOMCAT-GLOMAP to a best-estimate based on observed global surface mean concentration (McNorton et al., 2016a; Dlugokencky, 2019). ~~Biogenic emissions are taken from MACCity and CCMI (Chemistry-Climate Model Initiative: http://www.met.reading.ac.uk/ccmi/). The CH_4 inventory is provided from a new emissions inventory derived from the Joint UK Land Environment Simulator (JULES), combined with biomass burning emissions from GFEDv4. Surface CH_4 concentrations are scaled annually within TOMCAT-GLOMAP to a best-estimate of observed global surface mean.~~

2.2 Radiative transfer model

Radiative effects of O_3 changes are calculated using an O_3 radiative kernel approach~~,~~ derived by Rap et al. (2015) using an offline version of the Edwards and Slingo (1996) radiative transfer model. This considers six bands in the shortwave (SW), nine bands in the longwave (LW) and uses a delta-Eddington two-stream scattering solver at all wavelengths (Rap et al., 2015). This version has been used extensively in conjunction with TOMCAT/GLOMAP for calculating radiative forcing from simulated distributions of several short-lived climate pollutants (SLCPs) including BC, O_3 and CH_4 (Spracklen et al., 2011; Riese et al., 2012; Rap et al., 2013; Richards et al., 2013; Rap et al., 2015).

2.3 Simulations

All simulations are performed for 1997-2014 with a four-year spin-up through 1993-1996. The control run (CTRL) allows all emissions and meteorology to vary throughout the modelled period. GFED biomass burning emission inventories began in 1997, therefore the 1993-1996 spin-up simulation uses repeating 1999 emissions instead, as the closest year of 'average' emissions, having excluded 1997 and 1998 due to the exceptionally high emissions in those years (Schultz et al., 2008).

To test the impact of El Niño events on atmospheric chemistry, we performed 4 simulations listed in Table 1. Where model simulations used "Fixed" parameters in Table 1, the year 2013 emissions or meteorology are specified as invariant throughout the simulation. This year is chosen as the ENSO-neutral case, due to it being the least active ENSO year during 1997-2014, with a maximum bimonthly multivariate ENSO index (MEI) magnitude of -0.4 and the only year without a single MEI value that could be considered an active El Niño or La Niña (Wolter and Timlin, 1993; Wolter and Timlin, 1998). Throughout this study, an El Niño event was taken to be ongoing if the MEI was greater than +1.0.We perform factorial simulations, in which we in turn fix global biomass burning emissions (FIREFIX) and global meteorology (METFIX) to the 'ENSO-neutral' case. An additional perturbed simulation was performed in order to examine the secondary impact of CO on CH_4 via oxidation changes, where only CO emissions from biomass burning were fixed (COFIX).

Table 1. Details of TOMCAT model simulations. All simulations are run for 1997-2014.

Simulation name~~I.D.~~	Meteorology	CO biomass burning emissions	All other biomass burning emissions
CTRL	Varying	Varying	Varying
METFIX	Fixed	Varying	Varying
FIREFIX	Varying	Fixed	Fixed
COFIX	Varying	Fixed	Varying

3 Model Evaluation

We have conducted a comprehensive evaluation of the TOMCAT-GLOMAP coupled model using aircraft observations, and data from ozone sondes and satellites. In general the model is able to capture absolute concentrations, global distribution and seasonal variations of major species including O_3, CO and CH_4. MOPITT satellite retrievals have been used to evaluate CO at 800hPa and 500hPa (Emmons et al., 2004) ~~which~~ and are shown in Fig. S1 and S2 respectively, along with a description of the satellite produce and the averaging kernels applied to the model output. TOMCAT performs similarly here as in Monks et al. (2017), underestimating CO concentrations in the Northern Hemisphere (NH) while overestimating peak concentrations in biomass burning regions, with a maximum difference of ~75ppb (Fig. S1 and S2). However, TOMCAT is able to reproduce seasonal variations in CO and locates peak CO accurately over East Asia and Central Africa.

TOMCAT was also compared with satellite observations of lower tropospheric (0-6km) O_3 from the Ozone Monitoring Instrument (OMI). These data were provided by the Rutherford Appleton Laboratory (RAL; data version fv0214) using an optimal estimation retrieval scheme which resolves O_3 in the 0-6km layer by exploiting information in the Hartley and Huggins uv bands. The scheme derives from that discussed by Miles et al. (2015) for another UV sounder GOME-2. TOMCAT representation of O_3 concentrations between 0-6 km in NH winter are slightly improved on the Monks et al. (2017) version, particularly in tropical and Southern Hemisphere (SH) concentrations (Fig. S3). However, there remains a general low bias in global O_3 of up to 10 Dobson Units (DU) in winter in regions such as the southern Atlantic Ocean.

TOMCAT ~~-~~O_3 has also been evaluated using sonde observations (Fig. 1 and S4) (Tilmes et al., 2011), with ~~TOMCAT~~ the model generally representing the vertical profiles and absolute concentrations of O_3 very well~~, at the majority of sites~~ with a normalised mean bias (NMB) of 1.1% across all sites at 700-1000 hPa and 2.1% at 300-700 hPA. The model capably simulates the seasonality of tropospheric O_3 (Fig. 1), with a maximum seasonal bias of 6.3% at 300-700 hPa in March-May. There is no apparent regional or latitudinal bias, although simulated concentrations are significantly over-estimated in India (Fig. S4). In addition, the TOMCAT simulated global tropospheric burden of O_3 in 2000 is 342 Tg which falls within the range of published value (Table 2).

We have also assessed the capability of TOMCAT-GLOMAP to simulate observed responses to El Niño events. Ziemke et al. (2010) derived an O_3 ENSO index using satellite observations, finding that for a +1K change in the Nino 3.4 index, there was a 2.4 DU increase in the OEI. In TOMCAT-GLOMAP, we calculate a 2.8 DU increase per +1K in the Nino 3.4, indicating a slightly larger but comparable response to El Niño events. The regional response of tropospheric O_3 to El Niño was evaluated against an analysis using various observations and a chemistry-climate model in Zhang et al. (2015). That study observed increased total O_3 column in the North Pacific, southern USA, north-eastern Africa and East Asia, with decreases over central Europe and the North Atlantic. All of these observed responses were present in TOMCAT-GLOMAP simulations, except with a slight increase in TOC in central Europe and a simulated decrease in Western Europe and East Atlantic (Fig. S5).

Commented [MR[1]: New figure added.

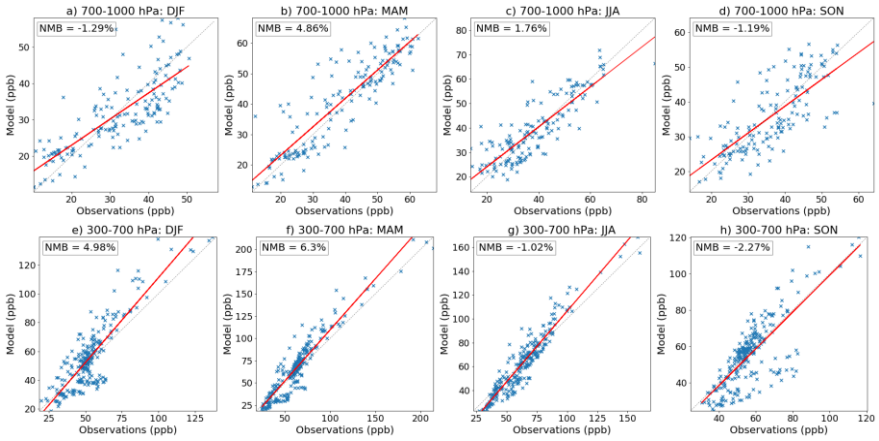

Figure 1: Comparison of seasonal mean simulated O_3 concentrations (ppb) against mean ozonesonde observations from Tilmes et al. (2012), for the period 1995-2011. Panels a-d show mean concentrations at 700-1000 hPa across all sites, while panels e-h show mean concentrations at 300-700 hPa. Values in each panel are seasonal means, from left to right, December-February (DJF), March-May (MAM), June-August (JJA) and September-November (SON). The red line represents the linear regression. Normalised mean bias (NMB) values between model and observations are also shown.

3.1 Aircraft observations

We compare annual mean simulated gas-phase species for 1999 against a climatological dataset of aircraft observations from 16 campaigns conducted from 1992 to 2001, with a broad spatial and temporal range (Emmons et al., 2010). While the comparison of observational data from intermittent aircraft campaigns does not offer a perfect comparison with the model simulated long-term mean concentrations, it allows evaluation of broad characteristics of a number of species over vertical profiles in many global regions. Figure ~~1~~2 shows the comparison of simulated annual mean global concentrations of O_3, CO, CH_4 and NO_x, with aircraft observations at 0- 2 km, 2-6 km and 6-10 km. We have also calculated the normalised mean bias between the model and observations (Fig. S6). Full details of the aircraft measurement campaigns used can be found in the Supplementary Table S1.

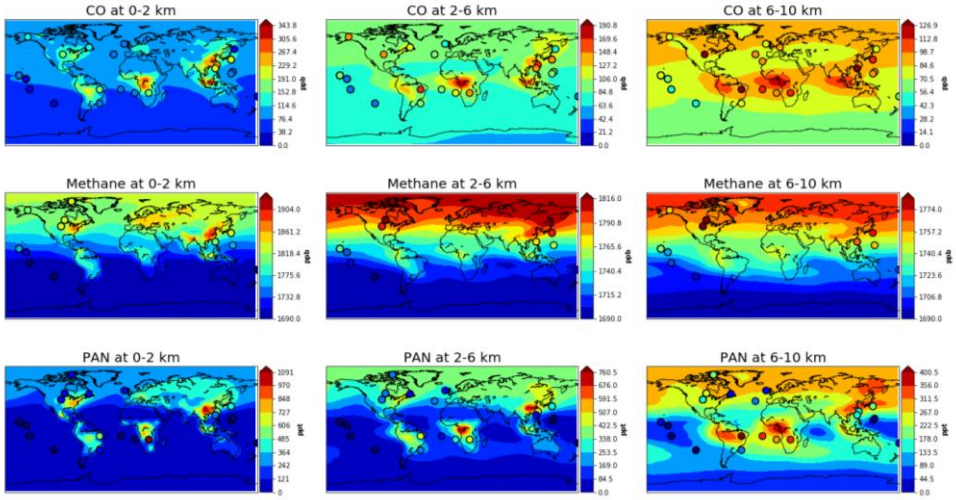

Figure ~~1~~2: Global ~~annual~~ mean volume mixing ratios of ~~O_3 (ppb),~~ CO (ppb), CH_4 (ppb) and ~~NO_x,~~ PAN (ppt) from TOMCAT for the period 1993-2001 at 0-2 km (left panels), 2-6 km (middle panels) and 6-10 km (right panels). The filled circles show mean values from aircraft observation~~s~~ campaigns which took place between 1992 and 2001 (Emmons et al., 2010).

~~The model tends to perform better near the surface level for all species, simulating higher concentrations in polluted urban or biomass burning regions, with lower concentrations over ocean and in the SH. O_3 concentrations increase with altitude which is well represented in TOMCAT, although values in the tropics are generally lower than the aircraft observations. CO concentrations decrease with altitude but highest values are still around urban areas and burning regions, which can be seen in both model and aircraft concentrations. Aircraft observations show CH_4 also decreases with altitude and the hemispherical disparity becomes more pronounced, with higher concentrations in the NH. Absolute concentrations in TOMCAT simulations match aircraft data very well and the latitudinal gradient is well captured. At 2-6 km and 6-10 km simulated concentrations are lower than observations at the majority of sites for NO_x. Given NO_x has a short lifetime of less than 1 day (Beirle et al., 2004; Liu et al., 2016), it is difficult for global models, such as TOMCAT, to reproduce observations due to their coarse horizontal and vertical resolutions (Huijnen et al., 2010).~~

The model captures broad characteristics of spatial distribution for all species, simulating higher concentrations in polluted urban or biomass burning regions, with lower concentrations over ocean and in the SH. CO concentrations decrease with altitude but the largest values still occur around urban areas and burning regions, which can be seen in both model and aircraft concentrations. Consistent with the comparison with MOPITT satellite retrievals (Fig. S1 and S2), the model underestimates

Commented [MR[2]: Table 1 now table 2 and has been edited.

CO concentrations particularly near the surface, with a NMB of -11.1%, -9.93% and -0.25% at 0-2 km, 2-6 km and 6-10 km, respectively. Absolute concentrations of CH_4 in TOMCAT simulations match aircraft data very well, although given the global mean surface concentration scaling we expect the magnitude of CH_4 to be well simulated. The latitudinal and vertical distributions are also well captured, giving confidence in the model transport and OH simulation. Aircraft observations show CH_4 also decreases with altitude and the hemispherical disparity becomes more pronounced, with higher concentrations in the NH. For PAN concentrations, the simulated spatial distribution is broadly well captured, as is the increased concentration with altitude. There is a general low bias in absolute concentrations near the surface (NMB=-12.3%), with better comparison at 2-6 km (NMB=1.68%) and over-estimation at 6-10 km (NMB=18.17%).

3.2 OH Evaluation

Due to the very short lifetime of OH, it is challenging to evaluate model simulated OH over representative spatial and temporal scales. Here we follow the evaluation methodology recommended by Lawrence et al. (2001), of dividing tropospheric OH into 12 sub-domains, from the surface to a climatologically derived tropopause. This methods ~~which~~ was also used to evaluate a previous version of TOMCAT (vn1.76) by Monks et al. (2017), allowing direct comparison. The evaluation is performed for the year 2000. Figure ~~2~~3 shows our simulated OH compared to Monks et al. (2017), the ACCMIP model mean (Naik et al., 2013) and the Spivakovsky et al. (2000) OH dataset estimated from methyl chloroform observations.

The models and observationally-constrained distribution broadly agree with the latitudinal spread of OH concentrations with a minimum in the SH and a maximum at the tropics; however there is disagreement over the exact altitude of the maximum OH concentrations. In both versions of TOMCAT the highest concentration is between the surface and 750hPa, while ACCMIP and Spivakovsky find peak OH in the upper and mid-level troposphere, respectively. The updated cloud fields used in the current TOMCAT-GLOMAP version have slightly increased OH concentrations in the mid-level and upper domains compared to Monks et al. (2017) but concentrations remain significantly higher in the NH and surface domains than in other studies. In addition, our simulated NH:SH ratio of 1.48 in the current TOMCAT version remains substantially higher than in the ACCMIP models (1.28 ± 0.1), indicating that TOMCAT photolysis rates and OH production in the NH are larger.

The total global tropospheric average OH in this version of TOMCAT is 1.04×10^6 molecules cm^{-3}, a decrease from Monks et al. (2017) and within the range of other published values (Table 2). This is primarily due an updated treatment of clouds, in which climatological cloud fields have been replaced with cloud fraction from ECMWF reanalyses data, affecting photolysis rates.The tropospheric O_3 burden of 342 Tg has increased relative to Monks et al. (2017) (331 Tg) and is within the range found in Wild (2007) (335 ± 10) and ACCMIP models (337 ± 23) (Young et al., 2013). ~~Due to the long lifetime of CH_4, its atmospheric lifetime cannot be determined from TOMCAT simulations.~~ Due to the simplified treatment of CH_4, the scaling applied and its relatively long atmospheric lifetime, the total atmospheric lifetime cannot be determined from TOMCAT simulations. Instead a chemical lifetime is calculated from CH_4 and OH burdens, disregarding stratospheric and soil sinks (Fuglestvedt et al., 1999; Berntsen et al., 2005; Voulgarakis et al., 2013). The lifetime diagnosed from TOMCAT is 8 years, compared to the multi-model mean and range of 9.3 ± 0.9 years from Voulgarakis et al. (2013). The shorter lifetime in TOMCAT is due to the overestimation of OH at the surface, particularly in the NH where CH_4 concentrations are highest due to anthropogenic emissions.

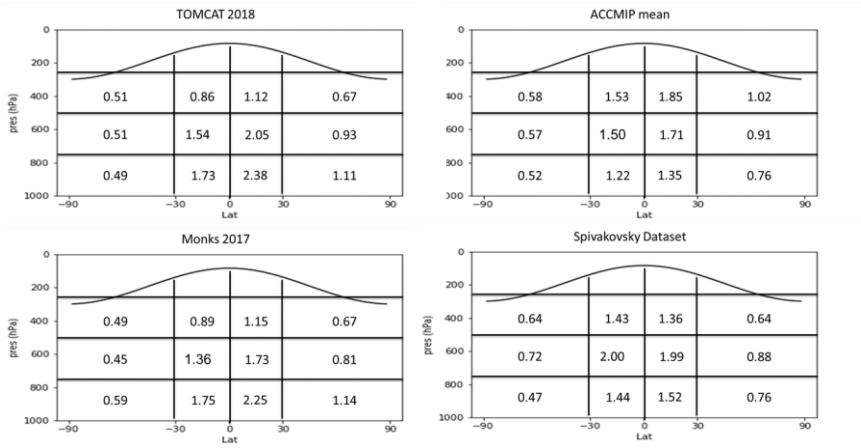

Figure 32: Annual zonal means of hydroxyl radical (OH) concentrations (×10^6 molecules cm^{-3}) divided into 12 sub-sections as recommended by Lawrence et al. (2001). The simulated OH from this study is compared to a dataset estimated from methyl chloroform observations (Spivakovsky et al., 2000) and the Atmospheric Chemistry and Climate Model Intercomparison Project (ACCMIP) multi-model mean (Naik et al., 2013). A previous version of TOMCAT from Monks et al. (2017) has also been included. A climatological tropopause, indicated by the smooth black line near the top of each panel, has been used to remove stratospheric OH.

Table 2: Present day (2000) TOMCAT model diagnostics compared to previous model version from Monks et al., (2017) and other published values.

Diagnostic	TOMCAT (this study)	Monks et al. (2017)	Other estimates	Reference
O_3 burden (Tg)	342	331	337 ± 23	Young et al. (2013)
Tropospheric OH concentration (×10^6 molecules cm^{-3})	1.04	1.08	0.94-1.06	Prinn et al. (2001); Krol and Lelieveld (2003); Bousquet et al. (2005); Wang et al. (2008).
CH_4 lifetime (years)	8.0	7.9	9.3 ± 0.9	Voulgarakis et al. (2013)

4 Results and discussion

4.1 Impact of meteorology and fire emissions on trace gas interannual variability

First we examine the mechanisms controlling interannual variability of simulated tropospheric CO, O_3 and mean OH. We use the difference between the control simulation (CTRL) and the perturbed simulations with fixed fires (FIREFIX) and fixed meteorology (METFIX) to determine the driving cause of IAV. Of particular interest is the effect of the 1997-1998 El Niño event (henceforth referred to as 1997 El Niño) and how the prevailing mechanisms controlling IAV change during such events. To define El Niño events, we use the bimonthly multivariate ENSO index, which is calculated from 6 observed variables and standardised to accurately monitor ENSO occurrence (Wolter and Timlin, 1998; Wolter and Timlin, 2011).

Previous studies examining the dominant factor controlling global CO IAV have found contrasting results. Szopa et al. (2007) suggested that meteorology was the main driver, accounting for 50-90% of IAV in the tropics. ~~In contrast, Voulgarakis et al. (2015) suggested that biomass burning was the much more dominant driver with only a small effect from meteorology. This assertion is further supported by the study of Monks et al. (2012) of CO IAV in the Arctic, where biomass was found to be dominant.~~ Conversely, a study by Monks et al. (2012) considered CO IAV in the Arctic, finding that biomass burning was the

dominant driver with a strong correlation to El Niño. Voulgarakis et al. (2015) also suggested that biomass burning was the more important driver of IAV with only a small effect from meteorology. Some of the differences in results can be explained by Szopa et al. (2007) considering only surface CO rather than the whole troposphere as in Voulgarakis et al. (2015). Here we also consider whole tropospheric CO and our results are in line with those from Voulgarakis et al. (2015). We find the dominant source of IAV across the entire period is emissions from biomass burning - indicated by the large difference between simulations CTRL and FIREFIX (Fig. ~~3~~4a), with a small effect from meteorological changes (CTRL – METFIX). This effect is largest during the 1997 El Niño where an increase in fire events increased CO concentrations by more than 40%. Smaller increases of 5.8% and 7.6% occur during less extreme El Niño events of ~~in~~ 2002/2003 and 2006, respectively, with only a 1.8% increase during ~~less extreme El Niño events, but the effect is not seen during~~ the 2009/2010 El Niño, indicating that El Niño only significantly impacts CO concentrations when there is an associated increase in global fire events.

Expanding on the work of Voulgarakis et al. (2015), we analysed IAV using a coefficient of variation (CV), calculated as the multi-year standard deviation normalised by the mean (Fig. ~~4~~5). The global annual mean CO IAV over the whole period is 11.0% for the whole troposphere, 14.3% for surface concentrations. This is in very good agreement with Voulgarakis et al. (2015) who calculated 10% IAV, and even better when we consider the same time period (2005-2009) when IAV decreases to 9.7%. The slightly lower estimate here may be a result of the fixed-year BVOC emissions, removing the effect of IAV of biogenic emissions on CO IAV. BVOC oxidation is estimated to contribute 15% of the total source of CO (Duncan et al., 2007), however the IAV of BVOC emissions has been found to be relatively small, ~2-4% (Naik et al., 2004; Lathière et al., 2005). Despite good global comparison with (Voulgarakis et al., 2015)~~However~~, there are regional differences; CO IAV from TOMCAT is much larger in high-latitude boreal regions. This is due to the difference in period studied meaning this study includes additional extreme events including unusually large Russia boreal wildfires in 2010 and 2012 (Gorchakov et al., 2014; Kozlov et al., 2014). Infrequent and extreme events such as these significantly increase IAV.

CO IAV is significantly greater in September-October, with peaks in known fire regions such as tropical South America, Africa, Southeast Asia and in boreal forests. This indicates a strong contribution of fire emissions to IAV especially from Indonesia (Fig. 4a), as also suggested by ~~the analysis of Fig. 3a and~~ previous studies (Monks et al., 2012; Huang et al., 2014; Voulgarakis et al., 2015). In the FIREFIX simulation IAV is ~55% of the CTRL value showing a large reduction in variability when interannual variability in fire emissions is removed. The IAV in March-April is significantly smaller than September-October as this period is outside the primary fire season for South America and Eurasia, although hotspots remain in Southeast Asia and Africa where fires commonly occur in March-April (van der Werf et al., 2017). Meteorology and atmospheric transport changes are most important in Africa in September-October and Indonesia in March-April (Fig. ~~4~~5c, d). Fire emissions occur in these regions but the meteorological effects are important sources of IAV. This is in good agreement with Voulgarakis et al. (2015) who found that with fixed biomass burning emissions, there remained high IAV over Africa during Dec-Jan, and Huang et al. (2014) who found CO over Central Africa correlated more closely with ice water content than CO emissions due to increased convective transport. However, the overall effect of meteorology on global IAV found here is much smaller than the 50-90% suggested by Szopa et al. (2007): when we consider only surface CO over the same period, fixing meteorology decreases the mean CO IAV by just 5%.

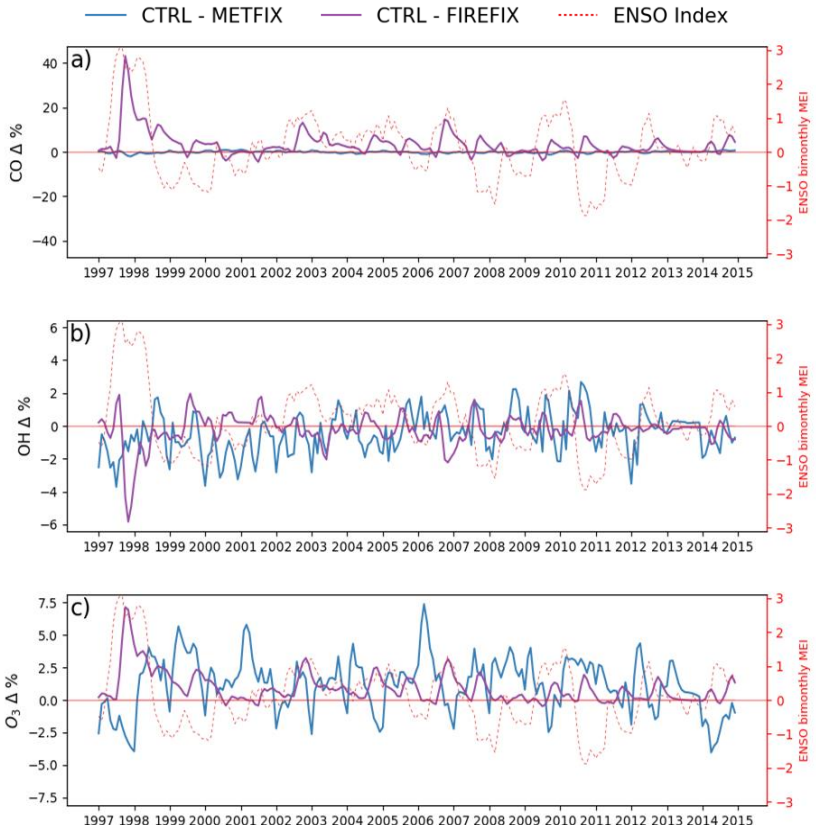

Figure ~~3~~4: Time series of simulated differences (%) between the control and the fixed meteorology (CTRL - METFIX, blue line) and fixed fire emissions (CTRL – FIREFIX, purple line) simulations for the global tropospheric burden of (a) CO, (b) OH and (c) O_3. The ENSO bimonthly mean multivariate index is plotted in the dashed red line on the right-hand ~~y-~~axis in each panel.

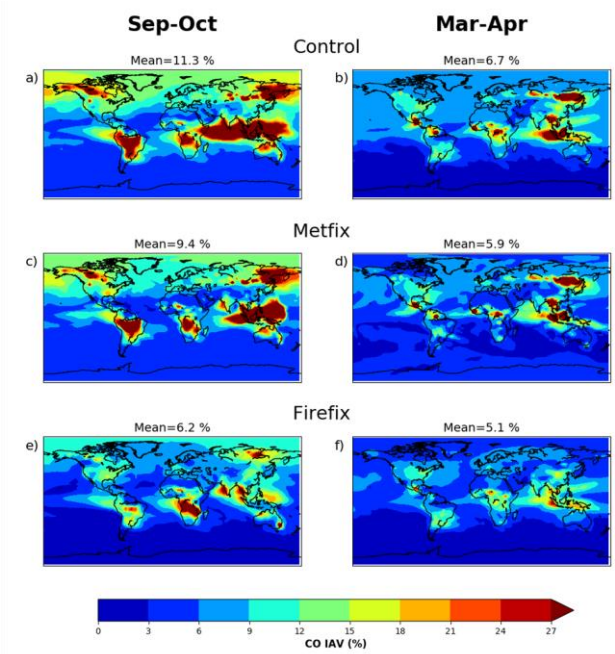

Figure 45: The calculated interannual variability (coefficient of variation) of CO over the period 1997-2014. Calculated for September – October (left panels) and March - April (right panels) for (a, b) control simulation (CTRL), (c, d) fixed meteorology (METFIX) and (e, f) fixed fire emissions (FIREFIX).

The IAV of OH and O_3 have more complex contributions from fire emissions and meteorology (Fig. 34b, c). For both species meteorology is the dominant cause of variability for the majority of the period, indicated by on-average greater deviation from CTRL in METFIX simulation than FIREFIX, including during El Niño events outside of the 1997 El Niño, such as in 2006. However, fire emissions are the dominant cause of variation during the 1997 El Niño for both species, increasing tropospheric O_3 burden by ~7% and decreasing tropospheric OH by ~6%. This indicates that while meteorology is the most important driver of IAV in global OH and tropospheric O_3, fire emissions also play a key role, sometimes even becoming the dominant driver when there are particularly large fire emissions during El Niño conditions. Our results compare well to Inness et al. (2015), who also found that changes to tropospheric O_3 during El Niño were driven by a combination of emissions and atmospheric dynamics. This is also in agreement with Doherty et al. (2006), where a strong correlation was found between ENSO meteorology and global O_3 burden, albeit with a lag period of several months. Various meteorological variables are known to affect OH and O_3 variability, including humidity, clouds and temperature (Stevenson et al., 2005; Holmes et al., 2013; Nicely et al., 2018). OH variability is particularly sensitive to changes in lightning NO_x production which decreases during El Niño conditions (Turner et al., 2018). Murray et al. (2014) also examined factors affecting OH variability since the last glacial maximum, finding tropospheric water vapour, overhead stratospheric O_3 and lightning NO_x to be key controlling factors. Furthermore, circulation changes during El Niño events have been linked to lower stratospheric O_3 variability (Zhang et al., 2015; Manatsa and Mukwada, 2017), which in turn influences tropospheric OH and O_3 concentrations (Holmes et al., 2013; Murray et al., 2014). Despite the importance of meteorological drivers, we find that fire emissions are the dominant cause of variation in both OH and O_3 during the 1997 El Niño, increasing global tropospheric O_3 burden by up to ~7% and decreasing tropospheric OH by up to ~6%. This result is supported by several other studies, which have found that during large fire events

such as that caused by the 1997 El Niño, fire emissions substantially decrease tropospheric OH and increase tropospheric O_3 (Hauglustaine et al., 1999; Sudo and Takahashi, 2001; Holmes et al., 2013). Our results indicate that while meteorology is generally the most important driver of IAV in global tropospheric OH and O_3, fire emissions can also play a key role and become the dominant driver when there are particularly large fire emissions related to El Niño.

Figure ~~5~~6 shows the IAV of O_3, supporting the analysis of Fig. 4 that also suggests meteorology is the dominant process in controlling IAV. METFIX-simulated IAV differs substantially from the CTRL, with much lower IAV in Sept-Oct (33% decrease) and in Mar-Apr (42% decrease) when meteorology is repeated. However, in the METFIX run there remain peaks in variability in close proximity to regions with large biomass burning emissions, demonstrating the significant contribution from fire emissions. In the FIREFIX simulation the distribution of IAV is broadly similar to the CTRL simulation and with only a small change in global mean CV, indicating that fire emissions have less control on O_3 IAV. These results are again comparable to Voulgarakis et al. (2015) as the distribution of O_3 IAV in both CTRL and FIREFIX simulations is similar although with slightly larger values of variation due to differing time period.

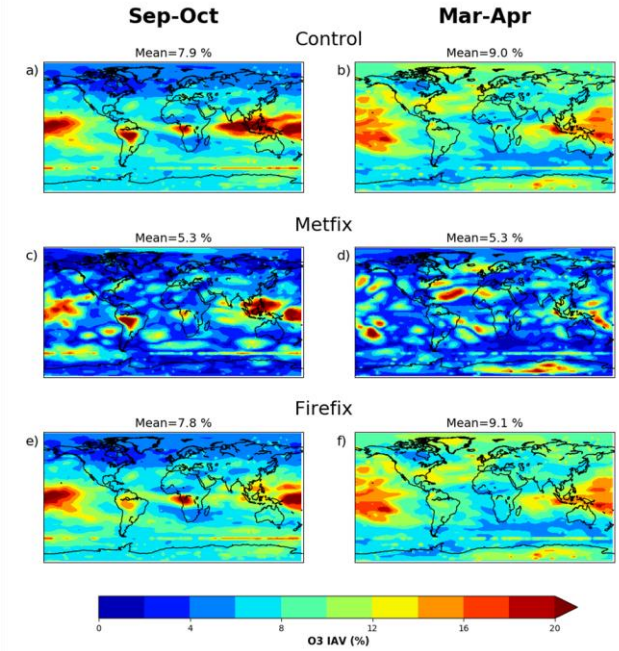

Figure ~~5~~6: The calculated interannual variability (coefficient of variation) of ozone over the period 1997 -2014. ~~Calculated~~ for September – October (left panels) and March - April (right panels) for (a, b) control simulation (CTRL), (c, d) fixed meteorology (METFIX) and (e, f) fixed fire emissions (FIREFIX).

4.2 Indirect effect of CO on oxidation and lifetime of CH_4

The COFIX sensitivity experiment was conducted to determine the indirect influence of CO emissions on CH_4 variability through changes in tropospheric OH concentrations. Figure ~~6~~7a shows the difference in COFIX monthly mean OH concentrations from the control experiment, compared to that from the METFIX and FIREFIX simulations. ~~Over the whole period, the inclusion of CO emissions from biomass burning consistently decreases tropospheric OH concentrations. This is due to the reaction of CO with OH which is the primary sink of CO.~~ When CO emissions from biomass burning are fixed, OH

concentrations are consistently higher than in the CTRL simulation. This indicates that high CO emissions decrease global mean tropospheric OH. The greatest impact is during the 1997 El Niño where CO emissions were abnormally large, suppressing mass weighted global monthly mean OH concentrations by up to 9%. The mean effect on OH over the 1997 El Niño of -3.6% is comparable to that simulated by Butler et al. (2005), who also found an increase in CO resulted in a change in OH of -2.2%. Duncan et al. (2003) found a similar magnitude response in OH to the Indonesian wildfires in 1997, of between -2.1% and -6.8%.~~This effect on OH in TOMCAT is considerably larger than that simulated by Butler et al. (2005), who also found an increase in CO during the 1997 El Niño and subsequent decrease OH of 2.2%.~~ The suppression of OH concentrations due to CO emission is also simulated to a lesser degree in the 2003 and 2006 El Niño events, but is absent in 2010 El Niño as this event had little impact on global fire occurrence (Randerson et al., 2017). The effect of fixing only CO from fires is greater than the effect of fixing all fire emissions due to co-emitted species such as NO_x, which act to increase OH concentrations.

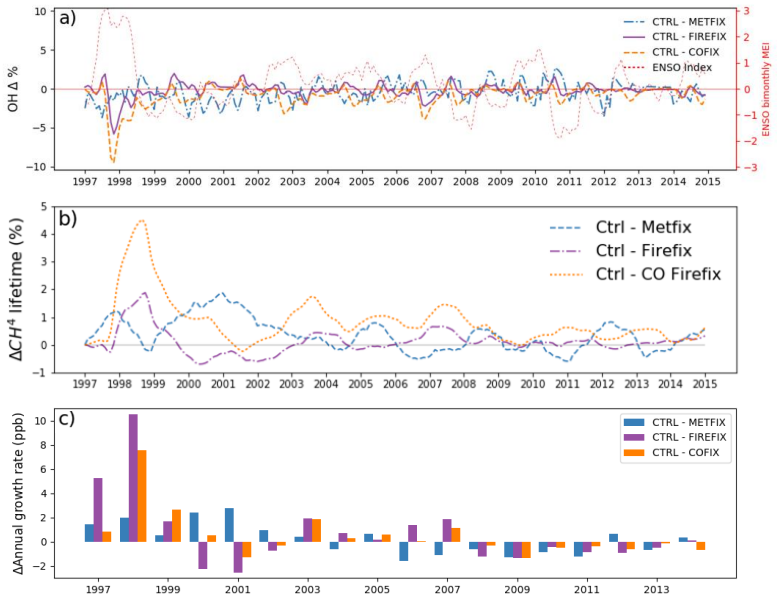

Figure ~~6~~7: Time series of (a) the change in mass-weighted tropospheric OH (%), (b) change in CH_4 lifetime (%) and (c) resultant change in annual growth rate calculated using an offline box model. The ENSO bimonthly mean multivariate index is plotted in the dashed red line on the right-hand y-axis in panel (a).

As OH is also the primary sink of CH_4 (~90%) (McNorton et al., 2016a), another effect of the decrease in OH due to CO emissions is to weaken the sink of CH_4, increasing its atmospheric lifetime. The magnitude of this can be seen in Fig. ~~6~~7b; the COFIX simulation indicates that CO emissions from fires extend CH_4 atmospheric lifetime by more than 4% during the 1997 El Niño. Fixing all fire emissions also enhances CH_4 lifetime by around 2%. Increasing the lifetime of a species increases its concentration in steady-state equilibrium. Due to the scaling applied to CH_4 in TOMCAT we are unable to directly calculate the response in CH_4 growth rate from TOMCAT, as simulated CH4 concentrations are nudged to the observed global mean surface value. Therefore, to determine the impact of the change to OH on CH_4 concentrations we used a simple global box model. This box model is similar to that described in McNorton et al. (2016a), which was found to compare well with other global and 12-box CH_4 models (Rigby et al., 2013; McNorton et al., 2016a). In this case, the box model used monthly mean tropospheric OH concentrations and CH_4 emissions for each simulation while assuming constant temperature to calculate the

effect of changing OH on global mean surface CH_4. . A fixed temperature was used as varying temperatures has been found to have a relatively small impact on derived CH_4 concentrations (McNorton et al., 2016a)The impact of fire emissions on the CH_4 growth rate is greatest in 1998, where all emissions from fires increased global CH_4 by 10.5 ppb (Fig. ~~6~~7c). Analysis of the COFIX simulation demonstrates that up to 7.5 ppb (72%) of that change could have been caused by the release of CO alone and its role as a sink for OH. The effect on growth rate in the FIREFIX simulation is larger than the COFIX despite a greater effect on CH_4 lifetime from the COFIX, due to directly emitted CH_4 varying with El Niño conditions in the COFIX simulation and not in FIREFIX. The influence of CO emissions on CH_4 growth rate calculated here is smaller than in Butler et al. (2005) despite a much larger effect on tropospheric OH. The radiative effect of the change to CH_4 from CO emitted from biomass burning alone in 1998 is 0.004 Wm^{-2}, calculated using updated expressions from Etminan et al. (2016).

4.3 Limiting factors of O_3 production

In this section we examine trends and the impact of El Niño on the production of tropospheric O_3. El Niño is known to have large effects on tropospheric O_3 precursors such as CO and NO_x, therefore examining O_3 production regimes during El Nino can provide insights into the main mechanism responsible for the observed changes in tropospheric O_3. The ratio between formaldehyde (HCHO) and nitrogen dioxide (NO_2) concentrations can be used to indicate the limiting factor for tropospheric O_3 production (Duncan et al., 2010). Ratios smaller than 1 indicate that removing VOCs will decrease tropospheric O_3 formation (i.e. a VOC-limited regime), while ratios larger than 2 indicate that removing NO_x will reduce O_3 (i.e. a NO_x-limited regime). Ratios of 1-2 indicate that both NO_x and VOC reductions could decrease O_3 (i.e. a 'both-limited' regime). Here we apply this methodology to determine the changes to this ratio from 1997-2014 and dependence of O_3 formation during the 1997 El Niño event. We compare the early period mean (199~~7~~9-200~~1~~3) to the end period mean (2010-2014) to determine whether significant changes have occurred over the 18-year period, and compared mean El Niño conditions to both.

In general, the SH and tropical regions have a very high ratios, meaning they are strongly NO_x-limited (Fig. ~~7~~8). The NH is also predominantly NO_x-limited although less robustly and polluted regions tend to be either VOC-limited or both-limited regimes. The ratio is largely constant across the modelled period, however there are some significant shifts such as in India, which was once solely NO_x-limited, becoming increasing VOC-limited due to increased NO_x pollution (Hilboll et al., 2017). This shift in the spatial distribution of O_3 precursor emissions to lower latitudes leads to increased tropospheric O_3 production proportional to total emissions (Zhang et al., 2016).

During El Niño there are large changes; increasing the ratio and therefore NO_x limitation by more than 40% in the Tropical Pacific. Significant changes to the ratio were also found in biomass burning regions of South America and Southeast Asia. This is due to the increase in NO_x emissions in larger fire seasons associated with El Niño. However, these regions are already very heavily NO_x-limited due to high VOC emissions in forest regions, meaning that although the shift in $HCHO/NO_2$ ratio during El Niño is large, it is not substantial enough to alter the limiting factor for formation of tropospheric O_3 from one regime to another. Over India, El Niño conditions inhibit the trend towards a "both-limited" regime, as the NO_x-limited regime continues to dominate throughout.

~~causes the solely NO_x-limited regime from the beginning of the period to persist throughout.~~

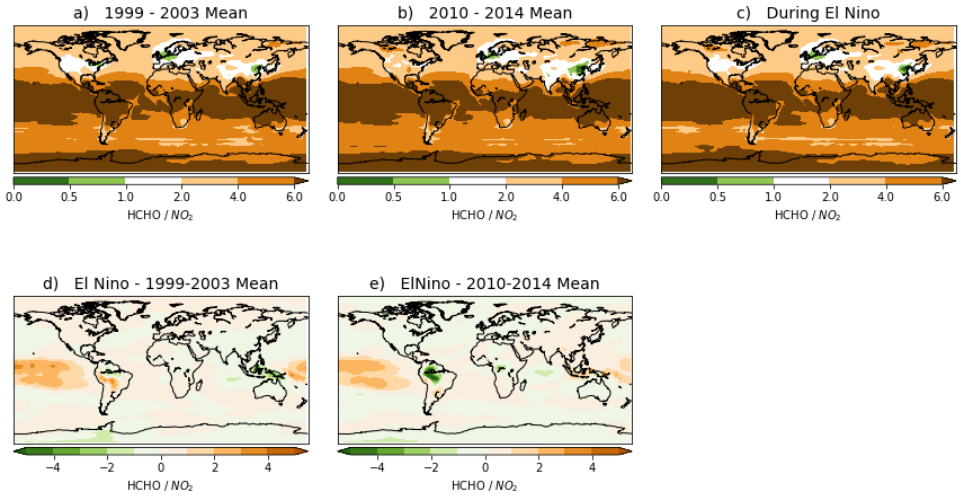

Figure ~~7~~8: 5-year mean of the ratio of tropospheric column HCHO to NO_2 at (a) the beginning of model period (1999-2003), (b) end of model period (2010-2014) and (c) mean ratio value during all El Niño events. Panels (d) and (e) show difference during El Niño from the 5-year mean values in panels (a) and (b), respectively.

4.4 Impact on tropospheric ozone and radiative effects

The 1997 El Niño significantly altered the vertical distribution of O_3 in the troposphere, increasing O_3 concentrations in the NH while decreasing in the SH and tropics with an overall decrease in tropospheric O_3 of -0.82% compared to the 1997-2014 mean (Fig. 9a). In the CTRL simulation there is decreased O_3 in the tropical upper troposphere, possibly related to increased convection over the Eastern Pacific (Oman et al., 2013; Neu et al., 2014). We also simulate large increases in the mid-latitude upper troposphere of both hemispheres in the CTRL and FIREFIX simulations but not in METFIX, implying that this is produced by El Niño-associated meteorological processes which promote intrusion of stratospheric air into the troposphere. These positive anomalies were also observed in Oman et al. (2013) and Zeng and Pyle (2005), attributed to El Niño influence on circulation patterns and enhanced stratospheric-troposphere exchange.

In general, the METFIX run simulates higher O_3 concentrations in the NH than the period mean and lower concentrations in the SH (Fig. 9b). This hemispherical shift is also present in the CTRL and FIREFIX simulations but with greater negative O_3 anomalies in the SH. The simulated NH increases in the CTRL simulation correspond to other studies of the 1997 El Niño (Koumoutsaris et al., 2008), while Oman et al. (2013) similarly reported negative O_3 anomalies in the SH during El Niño. Large increases in tropospheric O_3 in the Western Pacific, Indian Ocean and Europe contribute to the increase in O_3 in the NH, despite decreased O_3 in the Eastern Pacific (Chandra et al., 1998; Koumoutsaris et al., 2008; Oman et al., 2011).

There is an overall increase in O_3 (~2%) when meteorology was fixed to an ENSO-neutral year (i.e. 2013), meaning that meteorology during the 1997 El Niño caused a decrease in tropospheric O_3 concentrations despite large increases in O_3 in regions of the upper troposphere due to stratospheric intrusion. During the 1997 El Niño we find a 0.4% increase in global tropospheric humidity compared to the period mean. This is likely partly responsible for the general decrease in O_3 due to meteorology, as increased humidity enhances O_3 loss (Stevenson et al., 2000; Isaksen et al., 2009; Kawase et al., 2011). Changes to transport and distribution of O_3 will also impact how efficiently tropospheric O_3 is produced and lost.

The similarities between the tropospheric O_3 distribution in the CTRL and FIREFIX simulations show that fire emissions have a relatively small impact on the global distribution of O_3, but do affect absolute values, as concentrations in the FIREFIX run

are significantly lower at the tropics. This is likely because of the removal of large emissions of O_3 precursors in that latitude band when fire emissions are fixed to a non-El Niño year, as several studies have found that enhanced fires in 1997 El Niño increased tropospheric O_3 in the region (Chandra et al., 1998; Thompson et al., 2001; Doherty et al., 2006; Oman et al., 2013). ~~The 1997 El Niño significantly altered the vertical distribution of O_3 in the troposphere – increasing O_3 concentrations in the NH while decreasing in the SH and tropics with an overall decrease in tropospheric O_3 of -0.82% compared to the 1997-2014 mean (Fig. 8a). There are also very large increases in the mid-latitude upper troposphere of both hemispheres in the CTRL and FIREFIX simulations but not in METFIX, implying that this is produced by El Niño-associated meteorological processes which promote intrusion of stratospheric air into the troposphere. In general the METFIX run simulates much higher O_3 concentrations in the NH than the period mean and lower concentrations in the SH (Fig. 8b). There is an overall increase in O_3 (~2%) when meteorology was fixed to an ENSO-neutral year (i.e. 2013), meaning that meteorology during the 1997 El Niño caused a decrease in tropospheric O_3 concentrations despite large increases in O_3 in regions of the upper troposphere due to stratospheric intrusion. In the 1997 El Niño we find a 0.4% increase in global tropospheric humidity compared to the period mean. This is likely responsible for the decrease in O_3 due to meteorology as increased humidity enhances O_3 loss (Stevenson et al., 2000; Isaksen et al., 2009; Kawase et al., 2011). Changes to transport and distribution of O_3 will also impact how effectively tropospheric O_3 is produced and lost.~~

~~The similarities between the tropospheric O_3 distribution in the CTRL and FIREFIX simulations shows that fire emissions have a relatively small impact on the global distribution of O_3, but do affect absolute values, as concentrations in the FIREFIX run are significantly lower at the tropics. This is likely because of the removal of large emissions of O_3 precursors in that latitude band when fire emissions are fixed to a non-El Niño year.~~

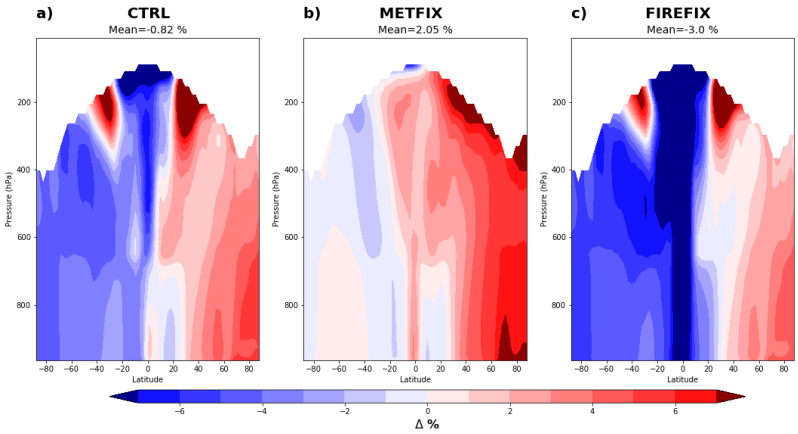

Figure ~~8~~9: Latitude-pressure ~~profiles~~ cross sections of the percentage difference in O_3 concentration during 1997 El Niño event compared to 1997-2014 period mean for simulations (a) CTRL, (b) METFIX and (c) FIREFIX.

Figure 910 shows the tropospheric O_3 radiative effect (RE) during the 1997 El Niño in each TOMCAT simulation, calculated using the Rap et al. (2015) tropospheric O_3 radiative kernel. Consistent with the relative changes in O_3 concentration, fire emissions and meteorology have contrasting effects on O_3 RE. When isolated, these effects are opposite and almost equal: fire emissions increase O_3 RE by 0.031 Wm^{-2} while meteorology decreases by -0.030 Wm^{-2}. We performed an additional simulation to determine the effect of these factors occurring simultaneously (BOTHFIX) - and found the increasing effect from fire emissions to be dominant over the decreasing effect from meteorology, leading to an overall increase in global mean O_3 RE of 0.015 W m^{-2}.

The effect of fire emissions occurs almost entirely over Indonesia and the Eastern Indian Ocean where the large influx of NO_x, CO, CH_4 and other O_3 precursors from fire emissions during the 1997 El Niño causes regional increases in tropospheric O_3 RE of up to 0.17 Wm^{-2}. Meteorology has more varied impacts during El Niño; causing large decreases in O_3 RE over the Central Pacific Ocean (~ -0.36 Wm^{-2}) but also increases in the mid-latitudes of the Pacific Ocean (~0.33 Wm^{-2}). Globally the mean change to O_3 RE is small, around 0.015 Wm^{-2}, but large regional changes have the potential to significantly alter atmospheric heating and dynamics.

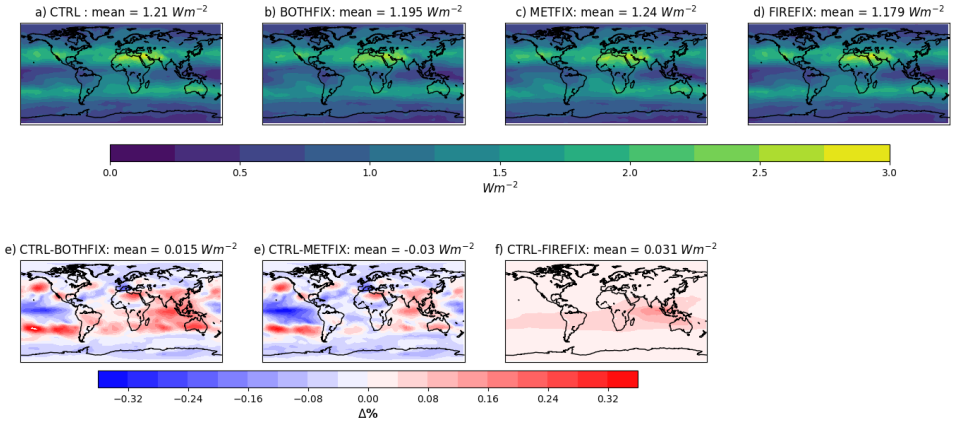

Figure ~~9~~10: Tropospheric O_3 radiative effects (Wm^{-2}) from the TOMCAT simulations (a) control, (b) fixed meteorology and fixed fire emissions, (c) fixed meteorology only and (d) fixed fire emissions only (d). Panels (e-g) show percentage differences between the control and the three perturbed simulations.

6 Summary and conclusions

Global model simulations using annually invariant meteorology and fire emissions were performed for the period 1997-2014 in order to determine their relative impacts on IAV of O_3 and CH_4, particularly during El Nino events. The TOMCAT-GLOMAP model used has been updated compared to that described by Monks et al. (2017) with improved cloud and photolysis representation and the introduction of Martensson sea spray emissions (Gordon et al., 2017). Model simulations were evaluated for a number of chemical species (O_3, CH_4, NO_x, CO) with observations from aircraft, satellites and ozone sondes. In general, the model shows a reasonable agreement with observed values although there are some regional and seasonal biases. Differences between model and observations may be due to a number of factors, such as the relatively coarse model resolution, uncertainties in the model emission inventories and errors in observations. However, good overall agreement of model simulations with different observations, including the ability of the model to simulate the observed atmospheric responses to El Niño events (i.e. OEI change of 2.8 DU compared to 2.4 DU in Ziemke et al. (2010)), provides confidence in model performance and results. ~~Differences between model and observations may be due to numbers of factors such as the relatively coarse model resolution, uncertainties in the model emission inventories and errors in observations. However, good overall agreement of model simulations with multiple observations gives us the confidence in model performance to support the results.~~

The IAV of global CO concentrations is large and are primarily controlled by fire emissions over the modelled period. Exceptionally large CO emissions linked to El Niño in 1997 led to a decrease in OH concentrations of ~9%, which subsequently increased CH_4 lifetime by ~4%. Using a box model we quantify the isolated impact of this change in atmospheric chemistry

on global CH_4 growth rate to be 7.75 ppb, ~75% of the total effect of fires. This effect, combined with concurrent direct CH_4 emission from fires explains the observed changes to CH_4 growth rate during the 1997 El Niño.

Variability of oxidants O_3 and OH is far more dependent on meteorology than fire emissions, except during very large El Niño events such as in 1997 and 1998, when fires become dominant in terms of total tropospheric burden although meteorology still controls distribution. The change to tropospheric O_3 concentrations during El Niño has increased O_3 RF by 0.17 Wm^{-2} over Southeast Asia and decreased by 0.36 Wm^{-2} over the Central Pacific. The global mean O_3 RF change due to 1997 El Niño meteorology and fires is an increase of 0.015 Wm^{-2}, as emissions of O_3 precursors from fires causes increased O_3. El Niño also causes significant shifts in the ratio of $HCHO/NO_x$ – an indicator of O_3 production regime – but most significantly in the tropics which are heavily NO_x-limited, so this change does not cause a regime shift.

We have shown that El Niño events significantly affect the variability of two important drivers of anthropogenic climate change. Further research into how El Niño events, and their effect on fire emissions, is likely to change in a warming climate is required to understand how these links between ENSO and CH_4 and O_3 may change and influence future climate change mitigation attempts.

Author contribution

MR, AR and SA conceptualised the study and planned the experiments. MC, KP, HG, WF and MR developed and evaluated the version of TOMCAT-GLOMAP used here. BK, BL and RS provided the satellite retrievals for the O_3 comparison which was conducted by RP. MC and JM provided assistance and advice for the CH_4 box model. MR performed the TOMCAT model runs, SOCRATES and box model calculations. MR analysed the results with help from AP and SA. MR compiled results and prepared the manuscript. All co-authors contributed to the final version with comments.

Acknowledgements

M. Rowlinson is funded by a studentship for the NERC SPHERES Doctoral Training Partnership (NE/L002574/1). This work was undertaken using the ARCHER UK National Supercomputing Service (http://www.archer.ac.uk) and ARC3, part of the High Performance Computing facilities at the University of Leeds, UK.

References

Anenberg, S. C., Horowitz, L. W., Tong, D. Q., and West, J. J.: An Estimate of the Global Burden of Anthropogenic Ozone and Fine Particulate Matter on Premature Human Mortality Using Atmospheric Modeling, Environmental Health Perspectives, 118, 1189-1195, doi:10.1289/ehp.0901220, 2010.

Beirle, S., Platt, U., von Glasow, R., Wenig, M., and Wagner, T.: Estimate of nitrogen oxide emissions from shipping by satellite remote sensing, Geophysical Research Letters, 31, doi:10.1029/2004GL020312, 2004.

Berntsen, T. K., Fuglestvedt, J. S., Joshi, M. M., Shine, K. P., Stuber, N., Ponater, M., Sausen, R., Hauglustaine, D. A., and Li, L.: Response of climate to regional emissions of ozone precursors: sensitivities and warming potentials, Tellus B: Chemical and Physical Meteorology, 57, 283-304, 10.3402/tellusb.v57i4.16549, 2005.

Bousquet, P., Hauglustaine, D. A., Peylin, P., Carouge, C., and Ciais, P.: Two decades of OH variability as inferred by an inversion of atmospheric transport and chemistry of methyl chloroform, Atmos. Chem. Phys., 5, 2635-2656, 10.5194/acp-5-2635-2005, 2005.

Bousquet, P., Ciais, P., Miller, J. B., Dlugokencky, E. J., Hauglustaine, D. A., Prigent, C., Van der Werf, G. R., Peylin, P., Brunke, E. G., Carouge, C., Langenfelds, R. L., Lathière, J., Papa, F., Ramonet, M., Schmidt, M., Steele, L. P., Tyler, S. C., and White, J.: Contribution of anthropogenic and natural sources to atmospheric methane variability, Nature, 443, 439, 10.1038/nature05132
https://www.nature.com/articles/nature05132#supplementary-information, 2006.

Butler, T. M., Rayner, P. J., Simmonds, I., and Lawrence, M. G.: Simultaneous mass balance inverse modeling of methane and carbon monoxide, Journal of Geophysical Research: Atmospheres, 110, doi:10.1029/2005JD006071, 2005.

Chandra, S., Ziemke, J. R., Min, W., and Read, W. G.: Effects of 1997–1998 El Niño on tropospheric ozone and water vapor, Geophysical Research Letters, 25, 3867-3870, 10.1029/98GL02695, 1998.

Chen, Y.-H., and Prinn, R. G.: Estimation of atmospheric methane emissions between 1996 and 2001 using a three-dimensional global chemical transport model, Journal of Geophysical Research: Atmospheres, 111, doi:10.1029/2005JD006058, 2006.

Chipperfield, M. P.: New version of the TOMCAT/SLIMCAT off-line chemical transport model: Intercomparison of stratospheric tracer experiments, Quarterly Journal of the Royal Meteorological Society, 132, 1179-1203, doi:10.1256/qj.05.51, 2006.

Corbett, A., Jiang, X., Xiong, X., Kao, A., and Li, L.: Modulation of midtropospheric methane by El Niño, Earth and Space Science, 4, 590-596, doi:10.1002/2017EA000281, 2017.

Dee, D. P., Uppala, S. M., Simmons, A. J., Berrisford, P., Poli, P., Kobayashi, S., Andrae, U., Balmaseda, M. A., Balsamo, G., Bauer, P., Bechtold, P., Beljaars, A. C. M., van de Berg, L., Bidlot, J., Bormann, N., Delsol, C., Dragani, R., Fuentes, M., Geer, A. J., Haimberger, L., Healy, S. B., Hersbach, H., Hólm, E. V., Isaksen, L., Kållberg, P., Köhler, M., Matricardi, M., McNally, A. P., Monge-Sanz, B. M., Morcrette, J.-J., Park, B.-K., Peubey, C., de Rosnay, P., Tavolato, C., Thépaut, J.-N., and Vitart, F.: The ERA-Interim reanalysis: configuration and performance of the data assimilation system, 137, 553-597, 10.1002/qj.828, 2011.

Dlugokencky, E.: NOAA/ESRL, (www.esrl.noaa.gov/gmd/ccgg/trends_ch4/), 2019.

Dlugokencky, E. J., Nisbet, E. G., Fisher, R., and Lowry, D.: Global atmospheric methane: budget, changes and dangers, Philosophical Transactions of the Royal Society A: Mathematical, Physical and Engineering Sciences, 369, 2058-2072, 10.1098/rsta.2010.0341, 2011.

Doherty, R. M., Stevenson, D. S., Johnson, C. E., Collins, W. J., and Sanderson, M. G.: Tropospheric ozone and El Niño–Southern Oscillation: Influence of atmospheric dynamics, biomass burning emissions, and future climate change, 111, 10.1029/2005jd006849, 2006.

Duncan, B., Yoshida, Y., R. Olson, J., Sillman, S., Martin, R., Lamsal, L., Hu, Y., E. Pickering, K., Retscher, C., and J. Allen, D.: Application of OMI observations to a space-based indicator of NOx and VOC controls on surface ozone formation, 2213-2223 pp., 2010.

Duncan, B. N., Bey, I., Chin, M., Mickley, L. J., Fairlie, T. D., Martin, R. V., and Matsueda, H.: Indonesian wildfires of 1997: Impact on tropospheric chemistry, 108, 10.1029/2002jd003195, 2003.

Duncan, B. N., Logan, J. A., Bey, I., Megretskaia, I. A., Yantosca, R. M., Novelli, P. C., Jones, N. B., and Rinsland, C. P.: Global budget of CO, 1988–1997: Source estimates and validation with a global model, 112, 10.1029/2007jd008459, 2007.

Emmons, L. K., Deeter, M. N., Gille, J. C., Edwards, D. P., Attié, J.-L., Warner, J., Ziskin, D., Francis, G., Khattatov, B., Yudin, V., Lamarque, J.-F., Ho, S.-P., Mao, D., Chen, J. S., Drummond, J., Novelli, P., Sachse, G., Coffey, M. T., Hannigan, J. W., Gerbig, C., Kawakami, S., Kondo, Y., Takegawa, N., Schlager, H., Baehr, J., and Ziereis, H.: Validation of Measurements of Pollution in the Troposphere (MOPITT) CO retrievals with aircraft in situ profiles, Journal of Geophysical Research: Atmospheres, 109, doi:10.1029/2003JD004101, 2004.

Emmons, L. K., Walters, S., Hess, P. G., Lamarque, J.-F., Pfister, G. G., Fillmore, D., Granier, C., Guenther, A., Kinnison, D., Laepple, T., Orlando, J., Tie, X., Tyndall, G., Wiedinmyer, C., Baughcum, S. L., and Kloster, S.: Description and evaluation of the Model for Ozone and Related chemical Tracers, version 4 (MOZART-4), Geoscientific Model Development, 3, 43-67, 10.5194/gmd-3-43-2010, 2010.

Etminan, M., Myhre, G., Highwood, E. J., and Shine, K. P.: Radiative forcing of carbon dioxide, methane, and nitrous oxide: A significant revision of the methane radiative forcing, Geophysical Research Letters, 43, 12,614-612,623, doi:10.1002/2016GL071930, 2016.

Feely, R. A., Gammon, R. H., Taft, B. A., Pullen, P. E., Waterman, L. S., Conway, T. J., Gendron, J. F., and Wisegarver, D. P.: Distribution of chemical tracers in the eastern equatorial Pacific during and after the 1982–1983 El Niño/Southern Oscillation event, Journal of Geophysical Research: Oceans, 92, 6545-6558, doi:10.1029/JC092iC06p06545, 1987.

Fuglestvedt, J. S., Berntsen, T. K., Isaksen, I. S. A., Mao, H., Liang, X.-Z., and Wang, W.-C.: Climatic forcing of nitrogen oxides through changes in tropospheric ozone and methane; global 3D model studies, Atmospheric Environment, 33, 961-977, https://doi.org/10.1016/S1352-2310(98)00217-9, 1999.

Gorchakov, G. I., Sitnov, S. A., Sviridenkov, M. A., Semoutnikova, E. G., Emilenko, A. S., Isakov, A. A., Kopeikin, V. M., Karpov, A. V., Gorchakova, I. A., Verichev, K. S., Kurbatov, G. A., and Ponomareva, T. Y.: Satellite and ground-based monitoring of smoke in the atmosphere during the summer wildfires in European Russia in 2010 and Siberia in 2012, International Journal of Remote Sensing, 35, 5698-5721, 10.1080/01431161.2014.945008, 2014.

Gordon, H., Kirkby, J., Baltensperger, U., Bianchi, F., Breitenlechner, M., Curtius, J., Dias, A., Dommen, J., Donahue, N. M., Dunne, E. M., Duplissy, J., Ehrhart, S., Flagan, R. C., Frege, C., Fuchs, C., Hansel, A., Hoyle, C. R., Kulmala, M., Kürten, A., Lehtipalo, K., Makhmutov, V., Molteni, U., Rissanen, M. P., Stozkhov, Y., Tröstl, J., Tsagkogeorgas, G., Wagner, R., Williamson, C., Wimmer, D., Winkler, P. M., Yan, C., and Carslaw, K. S.: Causes and importance of new particle formation in the present-day and preindustrial atmospheres, Journal of Geophysical Research: Atmospheres, 122, 8739-8760, doi:10.1002/2017JD026844, 2017.

Granier, C., Müller, J.-F., and Brasseur, G.: The Impact of Biomass Burning on the Global Budget of Ozone and Ozone Precursors., in: Biomass Burning and Its Inter-Relationships with the Climate System, edited by: Innes J.L., B. M., Verstraete M.M., Springer, Dordrecht, 2000.

Hauglustaine, D. A., Brasseur, G. P., and Levine, J. S.: A sensitivity simulation of tropospheric ozone changes due to the 1997 Indonesian fire emissions, 26, 3305-3308, 10.1029/1999gl900610, 1999.

Hilboll, A., Richter, A., and Burrows, J. P.: NO2 pollution over India observed from space — the impact of rapid economic growth, and a recent decline, Atmos. Chem. Phys. Discuss., 2017, 1-18, 10.5194/acp-2017-101, 2017.

Hodson, E. L., Poulter, B., Zimmermann, N. E., Prigent, C., and Kaplan, J. O.: The El Niño–Southern Oscillation and wetland methane interannual variability, Geophysical Research Letters, 38, doi:10.1029/2011GL046861, 2011.

Holmes, C. D., Prather, M. J., Søvde, O. A., and Myhre, G.: Future methane, hydroxyl, and their uncertainties: key climate and emission parameters for future predictions, Atmos. Chem. Phys., 13, 285-302, 10.5194/acp-13-285-2013, 2013.

Holtslag, A. A. M., and Boville, B. A.: Local Versus Nonlocal Boundary-Layer Diffusion in a Global Climate Model, Journal of Climate, 6, 1825-1842, 10.1175/1520-0442(1993)006<1825:Lvnbld>2.0.Co;2, 1993.

Huang, L., Fu, R., and Jiang, J. H.: Impacts of fire emissions and transport pathways on the interannual variation of CO in the tropical upper troposphere, Atmos. Chem. Phys., 14, 4087-4099, 10.5194/acp-14-4087-2014, 2014.

Huijnen, V., Eskes, H. J., Poupkou, A., Elbern, H., Boersma, K. F., Foret, G., Sofiev, M., Valdebenito, A., Flemming, J., Stein, O., Gross, A., Robertson, L., D'Isidoro, M., Kioutsioukis, I., Friese, E., Amstrup, B., Bergstrom, R., Strunk, A., Vira, J., Zyryanov, D., Maurizi, A., Melas, D., Peuch, V. H., and Zerefos, C.: Comparison of OMI NO₂ tropospheric columns with an ensemble of global and European regional air quality models, Atmos. Chem. Phys., 10, 3273-3296, 10.5194/acp-10-3273-2010, 2010.

Inness, A., Benedetti, A., Flemming, J., Huijnen, V., Kaiser, J. W., Parrington, M., and Remy, S.: The ENSO signal in atmospheric composition fields: emission-driven versus dynamically induced changes, Atmos. Chem. Phys., 15, 9083-9097, 10.5194/acp-15-9083-2015, 2015.

Isaksen, I. S. A., Granier, C., Myhre, G., Berntsen, T. K., Dalsøren, S. B., Gauss, M., Klimont, Z., Benestad, R., Bousquet, P., Collins, W., Cox, T., Eyring, V., Fowler, D., Fuzzi, S., Jöckel, P., Laj, P., Lohmann, U., Maione, M., Monks, P., Prevot, A. S. H., Raes, F., Richter, A., Rognerud, B., Schulz, M., Shindell, D., Stevenson, D. S., Storelvmo, T., Wang, W. C., van Weele, M., Wild, M., and Wuebbles, D.: Atmospheric composition change: Climate–Chemistry interactions, Atmospheric Environment, 43, 5138-5192, https://doi.org/10.1016/j.atmosenv.2009.08.003, 2009.

Jones, C. D., Collins, M., Cox, P. M., and Spall, S. A.: The Carbon Cycle Response to ENSO: A Coupled Climate–Carbon Cycle Model Study, Journal of Climate, 14, 4113-4129, 10.1175/1520-0442(2001)014<4113:tccrte>2.0.co;2, 2001.

Kawase, H., Nagashima, T., Sudo, K., and Nozawa, T.: Future changes in tropospheric ozone under Representative Concentration Pathways (RCPs), 38, doi:10.1029/2010GL046402, 2011.

Kirschke, S., Bousquet, P., Ciais, P., Saunois, M., Canadell, J. G., Dlugokencky, E. J., Bergamaschi, P., Bergmann, D., Blake, D. R., Bruhwiler, L., Cameron-Smith, P., Castaldi, S., Chevallier, F., Feng, L., Fraser, A., Heimann, M., Hodson, E. L., Houweling, S., Josse, B., Fraser, P. J., Krummel, P. B., Lamarque, J.-F., Langenfelds, R. L., Le Quéré, C., Naik, V., O'Doherty, S., Palmer, P. I., Pison, I., Plummer, D., Poulter, B., Prinn, R. G., Rigby, M., Ringeval, B., Santini, M., Schmidt, M., Shindell, D. T., Simpson, I. J., Spahni, R., Steele, L. P., Strode, S. A., Sudo, K., Szopa, S., van der Werf, G. R., Voulgarakis, A., van Weele, M., Weiss, R. F., Williams, J. E., and Zeng, G.: Three decades of global methane sources and sinks, Nature Geoscience, 6, 813, 10.1038/ngeo1955
https://www.nature.com/articles/ngeo1955#supplementary-information, 2013.

Koumoutsaris, S., Bey, I., Generoso, S., and Thouret, V.: Influence of El Niño–Southern Oscillation on the interannual variability of tropospheric ozone in the northern midlatitudes, Journal of Geophysical Research: Atmospheres (1984–2012), 113, 10.1029/2007JD009753, 2008.

Kozlov, V. S., Yausheva, E. P., Terpugova, S. A., Panchenko, M. V., Chernov, D. G., and Shmargunov, V. P.: Optical–microphysical properties of smoke haze from Siberian forest fires in summer 2012, International Journal of Remote Sensing, 35, 5722-5741, 10.1080/01431161.2014.945010, 2014.

Krol, M., and Lelieveld, J.: Can the variability in tropospheric OH be deduced from measurements of 1,1,1-trichloroethane (methyl chloroform)?, Journal of Geophysical Research: Atmospheres, 108, doi:10.1029/2002JD002423, 2003.

Lamarque, J. F., Bond, T. C., Eyring, V., Granier, C., Heil, A., Klimont, Z., Lee, D., Liousse, C., Mieville, A., Owen, B., Schultz, M. G., Shindell, D., Smith, S. J., Stehfest, E., Van Aardenne, J., Cooper, O. R., Kainuma, M., Mahowald, N., McConnell, J. R., Naik, V., Riahi, K., and van Vuuren, D. P.: Historical (1850–2000) gridded anthropogenic and biomass burning emissions of reactive gases and aerosols: methodology and application, Atmos. Chem. Phys., 10, 7017-7039, 10.5194/acp-10-7017-2010, 2010.

Lathière, J., Hauglustaine, D. A., De Noblet-Ducoudré, N., Krinner, G., and Folberth, G. A.: Past and future changes in biogenic volatile organic compound emissions simulated with a global dynamic vegetation model, 32, 10.1029/2005gl024164, 2005.

Lawrence, M., Jöckel, P., and Kuhlmann, R.: What does the global mean OH concentration tell us?, 2001.

Liu, F., Beirle, S., Zhang, Q., Dörner, S., He, K., and Wagner, T.: NOx lifetimes and emissions of cities and power plants in polluted background estimated by satellite observations, Atmos. Chem. Phys., 16, 5283-5298, 10.5194/acp-16-5283-2016, 2016.

Manatsa, D., and Mukwada, G.: A connection from stratospheric ozone to El Niño-Southern Oscillation, Scientific Reports, 7, 5558, 10.1038/s41598-017-05111-8, 2017.

Mann, G., S. Carslaw, K., Spracklen, D., A. Ridley, D., T. Manktelow, P., Chipperfield, M., Pickering, S., and E. Johnson, C.: Description and evaluation of GLOMAP-mode: A modal global aerosol microphysics model for the UKCA composition-climate model, 2010.

Manning, M. R., Lowe, D. C., Moss, R. C., Bodeker, G. E., and Allan, W.: Short-term variations in the oxidizing power of the atmosphere, Nature, 436, 1001, 10.1038/nature03900
https://www.nature.com/articles/nature03900#supplementary-information, 2005.

Matthews, E., and Fung, I.: Methane emission from natural wetlands: Global distribution, area, and environmental characteristics of sources, 1, 61-86, 10.1029/GB001i001p00061, 1987.

McNorton, J., Chipperfield, M., Gloor, M., Wilson, C., Wuhu, F., Hayman, G., Rigby, M., B. Krummel, P., O'Doherty, S., Prinn, R., Weiss, R., Young, D., Dlugokencky, E., and Montzka, S. A.: Role of OH variability in the stalling of the global atmospheric CH4 growth rate from 1999 to 2006, 1-24 pp., 2016a.

McNorton, J., Gloor, E., Wilson, C., Hayman, G. D., Gedney, N., Comyn-Platt, E., Marthews, T., Parker, R. J., Boesch, H., and Chipperfield, M. P.: Role of regional wetland emissions in atmospheric methane variability, 43, 11,433-411,444, 10.1002/2016gl070649, 2016b.

McPhaden, M. J., Zebiak, S. E., and Glantz, M. H.: ENSO as an Integrating Concept in Earth Science, Science, 314, 1740-1745, 10.1126/science.1132588, 2006.

Meng, L., Paudel, R., G. M. Hess, P., and Mahowald, N.: Seasonal and inter-annual variability in wetland methane emissions simulated by CLM4Me' and CAM-chem and comparisons to observations of concentrations, 2015.

Miles, G. M., Siddans, R., Kerridge, B. J., Latter, B. G., and Richards, N. A. D.: Tropospheric ozone and ozone profiles retrieved from GOME-2 and their validation, Atmos. Meas. Tech., 8, 385-398, 10.5194/amt-8-385-2015, 2015.

Monks, S., R. Arnold, S., Hollaway, M., Pope, R., Wilson, C., Wuhu, F., Emmerson, K., J. Kerridge, B., Latter, B., M. Miles, G., Siddans, R., and P. Chipperfield, M.: The TOMCAT global chemical transport model v1.6: Description of chemical mechanism and model evaluation, 3025-3057 pp., 2017.

Monks, S. A., Arnold, S. R., and Chipperfield, M. P.: Evidence for El Niño–Southern Oscillation (ENSO) influence on Arctic CO interannual variability through biomass burning emissions, Geophysical Research Letters, 39, doi:10.1029/2012GL052512, 2012.

Murray, L. T., Mickley, L. J., Kaplan, J. O., Sofen, E. D., Pfeiffer, M., and Alexander, B.: Factors controlling variability in the oxidative capacity of the troposphere since the Last Glacial Maximum, Atmos. Chem. Phys., 14, 3589-3622, 10.5194/acp-14-3589-2014, 2014.

Myhre, G., Shindell, D., Bréon, F.-M., Collins, W., Fuglestvedt, J., Huang, J., Koch, D., Lamarque, J.-F., Lee, D., Mendoza, B., Nakajima, T., Robock, A., Stephens, G., Takemura, T., and Zhang, H.: Anthropogenic and Natural Radiative Forcing, in: Climate Change 2013: The Physical Science Basis. Contribution of Working Group I to the Fifth Assessment Report of the Intergovernmental Panel on Climate Change, edited by: Stocker, T. F., Qin, D., Plattner, G.-K., Tignor, M., Allen, S. K., Boschung, J., Nauels, A., Xia, Y., Bex, V., and Midgley, P. M., Cambridge University Press, Cambridge, United Kingdom and New York, NY, USA, 659–740, 2013.

Naik, V., Delire, C., and Wuebbles, D. J.: Sensitivity of global biogenic isoprenoid emissions to climate variability and atmospheric CO2, 109, 10.1029/2003jd004236, 2004.

Naik, V., Voulgarakis, A., Fiore, A. M., Horowitz, L. W., Lamarque, J. F., Lin, M., Prather, M. J., Young, P. J., Bergmann, D., Cameron-Smith, P. J., Cionni, I., Collins, W. J., Dalsøren, S. B., Doherty, R., Eyring, V., Faluvegi, G., Folberth, G. A., Josse, B., Lee, Y. H., MacKenzie, I. A., Nagashima, T., van Noije, T. P. C., Plummer, D. A., Righi, M., Rumbold, S. T., Skeie, R., Shindell, D. T., Stevenson, D. S., Strode, S., Sudo, K., Szopa, S., and Zeng, G.: Preindustrial to present-day changes in tropospheric hydroxyl radical and methane lifetime from the Atmospheric Chemistry and Climate Model Intercomparison Project (ACCMIP), Atmos. Chem. Phys., 13, 5277-5298, 10.5194/acp-13-5277-2013, 2013.

Neu, J. L., Flury, T., Manney, G. L., Santee, M. L., Livesey, N. J., and Worden, J.: Tropospheric ozone variations governed by changes in stratospheric circulation, Nature Geoscience, 7, 340, 10.1038/ngeo2138 https://www.nature.com/articles/ngeo2138#supplementary-information, 2014.

Nicely, J. M., Canty, T. P., Manyin, M., Oman, L. D., Salawitch, R. J., Steenrod, S. D., Strahan, S. E., and Strode, S. A.: Changes in Global Tropospheric OH Expected as a Result of Climate Change Over the Last Several Decades, 123, 10,774-710,795, 10.1029/2018jd028388, 2018.

Nisbet, E. G., Dlugokencky, E. J., Manning, M. R., Lowry, D., Fisher, R. E., France, J. L., Michel, S. E., Miller, J. B., White, J. W. C., Vaughn, B., Bousquet, P., Pyle, J. A., Warwick, N. J., Cain, M., Brownlow, R., Zazzeri, G., Lanoisellé, M., Manning, A. C., Gloor, E., Worthy, D. E. J., Brunke, E.-G., Labuschagne, C., Wolff, E. W., and Ganesan, A. L.: Rising atmospheric methane: 2007–2014 growth and isotopic shift, Global Biogeochemical Cycles, 30, 1356-1370, doi:10.1002/2016GB005406, 2016.

Oman, L. D., Ziemke, J. R., Douglass, A. R., Waugh, D. W., Lang, C., Rodriguez, J. M., and Nielsen, J. E.: The response of tropical tropospheric ozone to ENSO, 38, 10.1029/2011gl047865, 2011.

Oman, L. D., Douglass, A. R., Ziemke, J. R., Rodriguez, J. M., Waugh, D. W., and Nielsen, J. E.: The ozone response to ENSO in Aura satellite measurements and a chemistry-climate simulation, 118, 965-976, 10.1029/2012jd018546, 2013.

Prinn, R. G., Huang, J., Weiss, R. F., Cunnold, D. M., Fraser, P. J., Simmonds, P. G., McCulloch, A., Harth, C., Salameh, P., O'Doherty, S., Wang, R. H. J., Porter, L., and Miller, B. R.: Evidence for Substantial Variations of Atmospheric Hydroxyl Radicals in the Past Two Decades, Science, 292, 1882-1888, 10.1126/science.1058673, 2001.

Randerson, J. T., Van Der Werf, G. R., Giglio, L., Collatz, G. J., and Kasibhatla, P. S.: Global Fire Emissions Database, Version 4.1 (GFEDv4), in, ORNL Distributed Active Archive Center, 2017.

Rap, A., Scott, C. E., Spracklen, D. V., Bellouin, N., Forster, P. M., Carslaw, K. S., Schmidt, A., and Mann, G.: Natural aerosol direct and indirect radiative effects, Geophysical Research Letters, 40, 3297-3301, doi:10.1002/grl.50441, 2013.

Rap, A., Richards, N. A. D., Forster, P. M., Monks, S. A., Arnold, S. R., and Chipperfield, M. P.: Satellite constraint on the tropospheric ozone radiative effect, Geophysical Research Letters, 42, 5074-5081, doi:10.1002/2015GL064037, 2015.

Reddington, C. L., Morgan, W. T., Darbyshire, E., Brito, J., Coe, H., Artaxo, P., Marsham, J., and Spracklen, D. V.: Biomass burning aerosol over the Amazon: analysis of aircraft, surface and satellite observations using a global aerosol model, Atmos. Chem. Phys. Discuss., 2018, 1-32, 10.5194/acp-2018-849, 2018.

Richards, N. A. D., Arnold, S. R., Chipperfield, M. P., Miles, G., Rap, A., Siddans, R., Monks, S. A., and Hollaway, M. J.: The Mediterranean summertime ozone maximum: global emission sensitivities and radiative impacts, Atmos. Chem. Phys., 13, 2331-2345, 10.5194/acp-13-2331-2013, 2013.

Riese, M., Ploeger, F., Rap, A., Vogel, B., Konopka, P., Dameris, M., and Forster, P.: Impact of uncertainties in atmospheric mixing on simulated UTLS composition and related radiative effects, Journal of Geophysical Research: Atmospheres, 117, doi:10.1029/2012JD017751, 2012.

Rigby, M., Prinn, R. G., Fraser, P. J., Simmonds, P. G., Langenfelds, R. L., Huang, J., Cunnold, D. M., Steele, L. P., Krummel, P. B., Weiss, R. F., O'Doherty, S., Salameh, P. K., Wang, H. J., Harth, C. M., Mühle, J., and Porter, L. W.: Renewed growth of atmospheric methane, Geophysical Research Letters, 35, doi:10.1029/2008GL036037, 2008.

Rigby, M., Prinn, R. G., O'Doherty, S., Montzka, S. A., McCulloch, A., Harth, C. M., Mühle, J., Salameh, P. K., Weiss, R. F., Young, D., Simmonds, P. G., Hall, B. D., Dutton, G. S., Nance, D., Mondeel, D. J., Elkins, J. W., Krummel, P. B., Steele, L. P., and Fraser, P. J.: Re-evaluation of the lifetimes of the major CFCs and CH₃CCl₃ using atmospheric trends, Atmos. Chem. Phys., 13, 2691-2702, 10.5194/acp-13-2691-2013, 2013.

Rossow, W. B., and Schiffer, R. A.: Advances in Understanding Clouds from ISCCP, Bulletin of the American Meteorological Society, 80, 2261-2288, 10.1175/1520-0477(1999)080<2261:Aiucfi>2.0.Co;2, 1999.

Schultz, M. G., Heil, A., Hoelzemann, J. J., Spessa, A., Thonicke, K., Goldammer, J. G., Held, A. C., Pereira, J. M. C., and van het Bolscher, M.: Global wildland fire emissions from 1960 to 2000, Global Biogeochemical Cycles, 22, doi:10.1029/2007GB003031, 2008.

Sindelarova, K., Granier, C., Bouarar, I., Guenther, A., Tilmes, S., Stavrakou, T., Müller, J. F., Kuhn, U., Stefani, P., and Knorr, W.: Global data set of biogenic VOC emissions calculated by the MEGAN model over the last 30 years, Atmos. Chem. Phys., 14, 9317-9341, 10.5194/acp-14-9317-2014, 2014.

Sitch, S., Cox, P. M., Collins, W. J., and Huntingford, C.: Indirect radiative forcing of climate change through ozone effects on the land-carbon sink, Nature, 448, 791, 10.1038/nature06059 https://www.nature.com/articles/nature06059#supplementary-information, 2007.

Spivakovsky, C. M., Logan, J. A., Montzka, S. A., Balkanski, Y. J., Foreman-Fowler, M., Jones, D. B. A., Horowitz, L. W., Fusco, A. C., Brenninkmeijer, C. A. M., Prather, M. J., Wofsy, S. C., and McElroy, M. B.: Three-dimensional climatological

distribution of tropospheric OH: Update and evaluation, Journal of Geophysical Research: Atmospheres, 105, 8931-8980, doi:10.1029/1999JD901006, 2000.

Spracklen, D. V., Jimenez, J. L., Carslaw, K. S., Worsnop, D. R., Evans, M. J., Mann, G. W., Zhang, Q., Canagaratna, M. R., Allan, J., Coe, H., McFiggans, G., Rap, A., and Forster, P.: Aerosol mass spectrometer constraint on the global secondary organic aerosol budget, Atmos. Chem. Phys., 11, 12109-12136, 10.5194/acp-11-12109-2011, 2011.

Stevenson, D., Doherty, R., Sanderson, M., Johnson, C., Collins, B., and Derwent, D.: Impacts of climate change and variability on tropospheric ozone and its precursors, Faraday discussions, 130, 41-57; discussion 125-151, 519-124, 2005.

Stevenson, D. S., Johnson, C. E., Collins, W. J., Derwent, R. G., and Edwards, J. M.: Future estimates of tropospheric ozone radiative forcing and methane turnover — The impact of climate change, 27, 2073-2076, doi:10.1029/1999GL010887, 2000.

Sudo, K., and Takahashi, M.: Simulation of tropospheric ozone changes during 1997–1998 El Niño: Meteorological impact on tropospheric photochemistry, 28, 4091-4094, 10.1029/2001gl013335, 2001.

Szopa, S., Hauglustaine, D. A., and Ciais, P.: Relative contributions of biomass burning emissions and atmospheric transport to carbon monoxide interannual variability, Geophysical Research Letters, 34, doi:10.1029/2007GL030231, 2007.

Thompson, A. M., Witte, J. C., Hudson, R. D., Guo, H., Herman, J. R., and Fujiwara, M.: Tropical Tropospheric Ozone and Biomass Burning, 291, 2128-2132, 10.1126/science.291.5511.2128 %J Science, 2001.

Tilmes, S., Lamarque, J.-F., Emmons, L., Conley, A., G. Schultz, M., Saunois, M., Thouret, V., Thompson, A., Oltmans, S., Johnson, B., and Tarasick, D.: Ozonesonde climatology between 1995 and 2009: Description, evaluation and applications, 28747-28796 pp., 2011.

Turner, A. J., Fung, I., Naik, V., Horowitz, L. W., and Cohen, R. C.: Modulation of hydroxyl variability by ENSO in the absence of external forcing, 115, 8931-8936, 10.1073/pnas.1807532115 %J Proceedings of the National Academy of Sciences, 2018.

van der Werf, G. R., Randerson, J. T., Collatz, G. J., Giglio, L., Kasibhatla, P. S., Arellano, A. F., Olsen, S. C., and Kasischke, E. S.: Continental-Scale Partitioning of Fire Emissions During the 1997 to 2001 El Niño/La Niña Period, Science, 303, 73-76, 10.1126/science.1090753, 2004.

van der Werf, G. R., Randerson, J. T., Giglio, L., van Leeuwen, T. T., Chen, Y., Rogers, B. M., Mu, M., van Marle, M. J. E., Morton, D. C., Collatz, G. J., Yokelson, R. J., and Kasibhatla, P. S.: Global fire emissions estimates during 1997–2016, Earth Syst. Sci. Data, 9, 697-720, 10.5194/essd-9-697-2017, 2017.

Voulgarakis, A., Naik, V., Lamarque, J. F., Shindell, D. T., Young, P. J., Prather, M. J., Wild, O., Field, R. D., Bergmann, D., Cameron-Smith, P., Cionni, I., Collins, W. J., Dalsøren, S. B., Doherty, R. M., Eyring, V., Faluvegi, G., Folberth, G. A., Horowitz, L. W., Josse, B., MacKenzie, I. A., Nagashima, T., Plummer, D. A., Righi, M., Rumbold, S. T., Stevenson, D. S., Strode, S. A., Sudo, K., Szopa, S., and Zeng, G.: Analysis of present day and future OH and methane lifetime in the ACCMIP simulations, Atmos. Chem. Phys., 13, 2563-2587, 10.5194/acp-13-2563-2013, 2013.

Voulgarakis, A., and Field, R. D.: Fire Influences on Atmospheric Composition, Air Quality and Climate, Current Pollution Reports, 1, 70-81, 10.1007/s40726-015-0007-z, 2015.

Voulgarakis, A., Marlier, M. E., Faluvegi, G., Shindell, D. T., Tsigaridis, K., and Mangeon, S.: Interannual variability of tropospheric trace gases and aerosols: The role of biomass burning emissions, Journal of Geophysical Research: Atmospheres, 120, 7157-7173, doi:10.1002/2014JD022926, 2015.

Wang, J. S., McElroy, M. B., Logan, J. A., Palmer, P. I., Chameides, W. L., Wang, Y., and Megretskaia, I. A.: A quantitative assessment of uncertainties affecting estimates of global mean OH derived from methyl chloroform observations, Journal of Geophysical Research: Atmospheres, 113, doi:10.1029/2007JD008496, 2008.

Wild, O.: Modelling the global tropospheric ozone budget: exploring the variability in current models, Atmos. Chem. Phys., 7, 2643-2660, 10.5194/acp-7-2643-2007, 2007.

Wolter, K., and Timlin, M.: Monitoring ENSO in COADS with a seasonally adjusted principal component index, 17th Climate Diagnostics Workshop, Norman, OK, 1993, 52-57.

Wolter, K., and Timlin, M. S.: Measuring the strength of ENSO events: How does 1997/98 rank?, Weather, 53, 315-324, doi:10.1002/j.1477-8696.1998.tb06408.x, 1998.

Wolter, K., and Timlin, M. S.: El Niño/Southern Oscillation behaviour since 1871 as diagnosed in an extended multivariate ENSO index (MEI.ext), International Journal of Climatology, 31, 1074-1087, doi:10.1002/joc.2336, 2011.

Yan, X., Akiyama, H., Yagi, K., and Akimoto, H.: Global estimations of the inventory and mitigation potential of methane emissions from rice cultivation conducted using the 2006 Intergovernmental Panel on Climate Change Guidelines, 23, 10.1029/2008gb003299, 2009.

Young, P. J., Archibald, A. T., Bowman, K. W., Lamarque, J. F., Naik, V., Stevenson, D. S., Tilmes, S., Voulgarakis, A., Wild, O., Bergmann, D., Cameron-Smith, P., Cionni, I., Collins, W. J., Dalsøren, S. B., Doherty, R. M., Eyring, V., Faluvegi, G., Horowitz, L. W., Josse, B., Lee, Y. H., MacKenzie, I. A., Nagashima, T., Plummer, D. A., Righi, M., Rumbold, S. T., Skeie, R. B., Shindell, D. T., Strode, S. A., Sudo, K., Szopa, S., and Zeng, G.: Pre-industrial to end 21st century projections of tropospheric ozone from the Atmospheric Chemistry and Climate Model Intercomparison Project (ACCMIP), Atmos. Chem. Phys., 13, 2063-2090, 10.5194/acp-13-2063-2013, 2013.

Zeng, G., and Pyle, J. A.: Influence of El Niño Southern Oscillation on stratosphere/troposphere exchange and the global tropospheric ozone budget, 32, 10.1029/2004gl021353, 2005.

Zhang, J., Tian, W., Wang, Z., Xie, F., and Wang, F.: The Influence of ENSO on Northern Midlatitude Ozone during the Winter to Spring Transition, 28, 4774-4793, 10.1175/jcli-d-14-00615.1, 2015.

Zhang, Y., Cooper, O. R., Gaudel, A., Thompson, A. M., Nédélec, P., Ogino, S.-Y., and West, J. J.: Tropospheric ozone change from 1980 to 2010 dominated by equatorward redistribution of emissions, Nature Geoscience, 9, 875, 10.1038/ngeo2827 https://www.nature.com/articles/ngeo2827#supplementary-information, 2016.

Zhu, Q., Peng, C., Ciais, P., Jiang, H., Liu, J., Bousquet, P., Li, S., Chang, J., Fang, X., Zhou, X., Chen, H., Liu, S., Lin, G., Gong, P., Wang, M., Wang, H., Xiang, W., and Chen, J.: Interannual variation in methane emissions from tropical wetlands triggered by repeated El Niño Southern Oscillation, Global Change Biology, 23, 4706-4716, doi:10.1111/gcb.13726, 2017.

Ziemke, J. R., Chandra, S., Oman, L. D., and Bhartia, P. K.: A new ENSO index derived from satellite measurements of column ozone, Atmos. Chem. Phys., 10, 3711-3721, 10.5194/acp-10-3711-2010, 2010.